Enigmatic amphibians in Mid-Cretaceous amber were chameleon-like and had ballistic feeding

Authors: Juan D. Daza[1]*, Edward L. Stanley[2], Arnau Bolet[3,4], Aaron. M. Bauer[5], J. Salvador Arias[6], Andrej Čerňanský[7], Joseph J. Bevitt[8], Philip Wagner[9], Susan E. Evans[10].

Affiliations:

[1] Department of Biological Sciences, Sam Houston State University, Huntsville, Texas, United States.

[2] Department of Herpetology, Florida Museum of Natural History, Gainesville, Florida, United States.

[3] Institut Català de Paleontologia Miquel Crusafont, Universitat Autònoma de Barcelona, Cerdanyola del Vallès, Spain.

[4] School of Earth Sciences, University of Bristol, Bristol, United Kingdom.

[5] Department of Biology and Center for Biodiversity and Ecosystem Stewardship, Villanova University, Villanova, Pennsylvania, United States.

[6] Fundación Miguel Lillo, CONICET, San Miguel de Tucumán, Argentina

[7] Department of Ecology, Laboratory of Evolutionary Biology, Faculty of Natural Sciences, Comenius University in Bratislava, Bratislava, Slovakia

[8]Australian Centre for Neutron Scattering, Australian Nuclear Science and Technology Organisation, Sydney, Australia.

[9] Allwetterzoo Münster, Department of Research & Conservation, Münster, Germany.

[10] Department of Cell and Developmental Biology, University College London, London, United Kingdom.

*Corresponding author. E-mail: juand.daza@gmail.com

Abstract: Albanerpetontids are tiny enigmatic fossil amphibians, possessing a unique suite of characteristics, including scales, and specialized jaw and neck joints. Here we describe the first fully articulated, 3-D specimens of a new albanerpetontid, preserved in Cretaceous amber. They preserve skeletal and soft tissues, including an elongated median hyoid element, the tip of which remains embedded in a distal tongue-pad. This arrangement is remarkably similar to that of chameleons in which a long tongue can be projected rapidly. Our results thus suggest that albanerpetontids were sit-and-wait ballistic tongue feeders, extending the record of this specialized feeding mode by around 100 million years.

One Sentence Summary: Tiny mid-Cretaceous amphibians predate chameleons and salamanders in innovative ballistic tongue feeding mechanism.

Main Text: The extinct amphibian clade Albanerpetontidae is currently represented by five genera spanning a period of over 165 million years from the Middle Jurassic (*1*) to the Early Pleistocene (*2*), and a geographical range from North America (*3, 4*) through Europe (*5*) and central Asia (*6*) to Japan (*7*). To date, the only records from a southern (Gondwanan) continental mass, albeit marginal, are from Morocco (*8, 9*). A majority of albanerpetontid records comprise jaws and sculptured frontal bones (*5*), although Cretaceous localities (in Spain and Italy (*1, 10,*

11) and Japan (*7*)) have yielded more substantive material, some with associated soft tissue showing the presence of dermal scales (*10*). Originally classified as salamanders (*11, 12*), albanerpetontids are now considered a distinct lineage (*10, 13*). Nonetheless, many questions remain as to the anatomy, lifestyle, and relationships of these strange amphibians.

Here we describe a new genus and species of albanerpetontid from the amber deposits of Myanmar. The material includes a complete three-dimensional adult skull, a tiny juvenile skeleton originally identified as a putative stem-chameleon (*14*), and a partial adult postcranium. The exquisite preservation of both skeletal remains and soft tissues reveals important clues as to the morphological and ecological character of these enigmatic amphibians.

Amphibia Linnaeus 1758

Albanerpetontidae Fox & Naylor 1982

Yaksha perettii gen. et sp. nov.

lSID urn:lsid:zoobank.org:pub:0C8EC7C5-66D4-4144-917D-5BFA3704EFA4

Etymology. The generic name is derived from Yaksha, a Hindu mythical spirit, guardian of natural treasures hidden in the earth or tree roots. The specific epithet recognizes Dr. Adolf Peretti, director of the Peretti Museum Foundation, who discovered the fossil and has done fieldwork in Myanmar for the last 10 years.

Holotype. Peretti Museum Foundation, Switzerland (GRS-Ref-060829), a complete articulated skull (Figs. 1A, G–N, Fig. 2A–B, Fig. 3A–R).

Paratype. JZC Bu154 (Fig.1B, F and Figs. S2–S3, Fig. 2K in Daza et al. (*14*)) James Zigras Collection, juvenile specimen, housed at the American Museum of Natural History, New York, USA.

Referred material. Peretti Museum Foundation, Switzerland, GRS-Ref-27746, partial postcranial skeleton (Fig. S4).

Locality and horizon. GRS-Ref-060829 (holotype) and GRS-Ref-27746 (referred material) were ethically sourced from the Hukaung Valley, near Tanaing township, Myitkyina District, Kachin Province, Myanmar, and legally exported (supplementary text S1.1). The juvenile paratype, JZC Bu154, is recorded as being from approximately 100 km west of the Myitkyina district. Amber from these mines has been dated as early Cenomanian, around 99 million years ago (Ma), using U-Pb isotopes (*15*).

Diagnosis for genus and species. A genus and species of albanerpetontid distinguished by the following combination of characters: paired robust premaxillae with a dorsal boss, wide lateral lingual buttress, and elongate vertical suprapalatal pits (Fig. 3A–C); posteriorly bifurcate parietals bounding cranial fenestrations anteriorly and medially (Fig. 3D–E); triangular frontal with long broad-based internasal process, frontal anteroposterior length equal to maximum anteroposterior length of parietal (Fig. 3F–H), prefrontal facets extending posterior to mid-length of frontal, weakly developed midventral crest, and ventrolateral crests that meet in ventral midline; medium length parietal postorbital processes sculptured in their proximal half; separate prefrontal and lacrimal bones; nasal excluded from narial margin; trifurcate unpaired vomer;

dentition showing size heterodonty anteriorly, resulting in sinuous occlusal surface; small body size (supplementary text S2.1, Differential diagnosis).

The holotype (GRS-Ref-060829) is the first fully articulated three-dimensional skull of an albanerpetontid (Fig. 1A, G–N, supplementary text S2.2). It is 12.18 mm in overall length (snout tip to occiput), giving an estimated snout-pelvis length (SPL) of 52 mm (based on the proportions of *Celtedens ibericus* (*10*)). The new Myanmar skull reveals the presence of epipterygoids (misinterpreted in the Japanese *Shirerpeton*(*7*)) that form an integral part of the jaw suspension; a complete braincase with ossification of the pila antoticae; a palate with a large open pyriform fossa undivided by a median parasphenoid rostrum; a trifurcated unpaired vomer, with paired palatines and pterygoids, all lacking teeth; and a long median hyoid 'entoglossal' process (not homologous with that of lizards). There are no ossified ceratobranchial elements. GRS-Ref-060829 also preserves remnants of the original soft tissues, notably the anterior tongue pad, into which the tip of the 'entoglossal' process is embedded, and parts of the eyelids, palatal fascia, and jaw musculature.

The juvenile specimen, JZC Bu154 (Fig.1B–F, supplementary text S2.3), establishes the presence of a four digit manus, uncertain in other articulated specimens (*1, 10*), and curved ungual phalanges covered by claw sheaths. GRS-Ref-27746 (Fig. S4, supplementary text S2.4) demonstrates that the tripartite pelvis (pubis, ischium, and vertical ilium) was supported by two sacral ribs (unlike the single sacral typically found in lissamphibians). Moreover, the vertical iliac blade, like that of chameleons, suggests a deep pelvis that may have allowed the legs to be angled ventrally for climbing.

Most albanerpetontid species are represented by isolated bones, and data matrices for the group rely mainly on frontal and jaw characters. We ran an analysis using the most comprehensive recent data matrix (*7, 16*). In the possession of dorsal cranial fenestrae, *Yaksha* most closely resembles the older (120 Ma) Japanese *Shirerpeton* (*7*), but the phylogenetic analysis placed *Yaksha* as the sister taxon to *Shirerpeton* + either a clade of derived *Albanerpeton* species (Fig. 4A) or *Albanerpeton nexuosum*. Both *Yaksha* and *Shirerpeton* are thus nested within *Albanerpeton* as currently defined. However, we support the view that the single genus *Albanerpeton*, extending from the mid-Cretaceous of North America (~100 Ma (*3*)) to the Early Pleistocene of Italy (~2 Ma (*2*)), requires revision and subdivision(*7*), with the name *Albanerpeton* restricted to the type species, *A. inexpectatum*, and those Cenozoic species that consistently group closely with it (Fig. 4, Supplementary text S3.1, Figs. S5–S11).

As the relationships of albanerpetontids to extant amphibians (Lissamphibia), and the wider relationships of lissamphibians to fossil amphibians, are currently debated, we updated the coding for albanerpetontids, based on *Yaksha*, into four recent data matrices (*17-20*). Depending on the matrix used, albanerpetontids were placed as sister to Batrachia (frogs+ salamanders) within lepospondyls (*17*); as stem-Lissamphibia (*19*); nested within Lissamphibia (*18*); or nested in a clade comprising derived lepospondyls and lissamphibians (*20*). Nevertheless, all analyses placed albanerpetontids either as stem-or crown Lissamphibia (Fig. 4C–F). Frustratingly, the new data provided no resolution to the lepospondyl vs temnospondyl origin hypotheses (*20, 21*) (supplementary text S3.2, Figs. S13-16).

The paratype of *Yaksha* (JZC Bu154) was previously identified as a stem-chameleon(*14*), based mainly on the long 'entoglossal' hyoid process. In chameleons, this hyoid element is embedded in the base of the tongue, surrounded by collagenous sheaths (*22*) and a circular accelerator muscle (*23*). Contraction of the muscle, enhanced by an elastic storage and release effect from the wrapping sheaths (*22, 24*), propels the tongue and entoglossal process out of the mouth, extending the tongue at speeds of up to 500 m/s and to a distance of at least a body length (*22*). An analogous mechanism exists in some plethodontid salamanders where, as the tongue extends, the entire hyoid apparatus is folded into a bundle of cartilaginous rods that is projected out of the mouth again by circular protractor muscles (*24, 25*). The 'entoglossal' process of *Yaksha* (and other albanerpetontids (*1*)) is embedded into the remnant of the tongue pad (Fig. 2B), and suggests that albanerpetontids also had a ballistic feeding strategy (Fig. S1), plausibly using a similar combination of circular muscles and wrapping collagen. This interpretation of *Yaksha* as a chameleon analogue may help to explain some of the specialized features of albanerpetontids, including the complex neck and jaw joints, the long curved unguals covered in claw sheaths (Fig. S2), and the large forward-looking orbits. We therefore interpret *Yaksha* (and all albanerpetontids) as a sit-and-wait predator, living on or around trees, and using a ballistic tongue to catch small invertebrates. In external appearance, albanerpetontids probably resembled tiny lizards more than salamanders.

There is a corollary to this. Most lissamphibians employ a combination of lung breathing and cutaneous respiration. Lacking rib-mediated ventilation, these amphibians inflate their lungs by buccal pumping, using the hyoid apparatus to raise and depress the floor of the mouth (*12*). Plethodontid salamanders are lungless and rely on cutaneous gas exchange. This freed the hyoid

apparatus from its constraints (*26*), permitting modification for specialized tongue feeding. By analogy, this must also apply to albanerpetontids, given their derived hyoid anatomy. Although the possession of scales might seem contradictory, studies on scaled caecilians have revealed some capacity for cutaneous gas exchange (*27*). For miniaturized amphibians like albanerpetontids, it may have been sufficient.

The paratype of *Yaksha* (JZC Bu154) has a skull four times smaller than that of the miniaturized adult specimen of *Yaksha*. In amphibians, miniaturization is frequently coupled with direct development (*28*). The diminutive paratype of *Yaksha* may therefore indicate that albanerpetontids lacked a free-living larva.

Yaksha provides significant new morphological, functional, and phylogenetic data for this enigmatic Jurassic-Pleistocene clade. Albanerpetontids are revealed as specialized, sit-and-wait terrestrial predators, combining lifestyle features of miniaturized chameleons and plethodontid salamanders, and extending the history of ballistic tongue feeding by around 100 Ma, given molecular divergence estimates dating the origins of crown chameleons (*29*) and plethodontids (*30*) to the Late Cretaceous/Paleocene.

References and Notes:

1. G. McGowan, Albanerpetontid amphibians from the Lower Cretaceous of Spain and Italy: a description and reconsideration of their systematics. *Zool. J. Linn. Soc.* **135**, 1–32 (2002).

2. A. Villa, H. A. Blain, M. Delfino, The Early Pleistocene herpetofauna of Rivoli Veronese (Northern Italy) as evidence for humid and forested glacial phases in the Gelasian of Southern Alps. *Palaeogeogr. Palaeocl.* **490**, 393–403 (2018).

3. J. D. Gardner, The amphibian *Albanerpeton arthridion* and the Aptian-Albian biogeography of albanerpetontids. *Palaeontology* **42**, 529–544 (1999).

4. J. D. Gardner, D. G. DeMar, Mesozoic and Palaeocene lissamphibian assemblages of North America: a comprehensive review. *Palaeobiodivers. Palaeoenviron.* **93**, 459–515 (2013).

5. J. Gardner, M. Böhme, in *Vertebrate microfossil assemblages.,* J. Sankey, S. Baszio, Eds. (Indiana University Press, Bloomington and Indianapolis, 2008), pp. 178-218.

6. P. Skutschas, New species of albanerpetontid amphibian from the Upper Cretaceous of Uzbekistan. *Acta Paleontol. Pol.* **52**, 819–821 (2007).

7. R. Matsumoto, S. E. Evans, The first record of albanerpetontid amphibians (Amphibia: Albanerpetontidae) from East Asia. *Plos One* **13**, (2018).

8. J. D. Gardner, S. E. Evans, D. Sigogneau-Russell, New albanerpetontid amphibians from the Early Cretaceous of Morocco and Middle Jurassic of England. *Acta Palaeontol. Pol.* **48**, 301–319 (2003).

9. H. Haddoumi *et al.*, Guelb el Ahmar (Bathonian, Anoual Syncline, eastern Morocco): First continental flora and fauna including mammals from the Middle Jurassic of Africa. *Gondwana Res.* **29**, 290–319 (2016).

10. G. McGowan, S. Evans, Albanerpetontid amphibians from the early Cretaceous of Spain. *Nature* **373**, 143–145 (1995).

11. R. Estes, *Handbuch der Palaoherpetologie, 2. Gymnophiona, Caudata*. P. Wellnhofer, Ed., (Gustav Fischer Verlag, Stuttgart, New York, 1981).

12. W. E. Duellman, L. Trueb, *Biology of Amphibians*. (Johns Hopkins University Press, Baltimore, 1994).

13. R. C. Fox, B. G. Naylor, A reconsideration of the relationships of the fossil amphibian Albanerpeton. *Can. J. of Earth Sci.* **19**, 118–128 (1982).

14. J. D. Daza, E. L. Stanley, P. Wagner, A. M. Bauer, D. A. Grimaldi, Mid-Cretaceous amber fossils illuminate the past diversity of tropical lizards. *Sci. Adv.* **2**, e1501080 (2016).

15. G. H. Shi *et al.*, Age constraint on Burmese amber based on U-Pb dating of zircons. *Cretac. Res.* **37**, 155–163 (2012).

16. S. C. Sweetman, J. D. Gardner, A new albanerpetontid amphibian from the Barremian (Early Cretaceous) Wessex Formation of the Isle of Wight, southern England. *Acta Palaeontol. Pol.* **58**, 295–324 (2013).

17. A. Huttenlocker, J. Pardo, B. J. Small, J. Anderson, Cranial morphology of recumbirostrans (Lepospondyli) from the Permian of Kansas and Nebraska, and early morphological evolution inferred by Micro-Computed Tomography. *J. Vert. Paleontol.* **33**, 540–552 (2013).

18. J. D. Pardo, M. Szostakiwskyj, P. E. Ahlberg, J. S. Anderson, Hidden morphological diversity among early tetrapods. *Nature* **546**, 642–645 (2017).

19. J. D. Pardo, B. J. Small, A. K. Huttenlocker, Stem caecilian from the Triassic of Colorado sheds light on the origins of Lissamphibia. *Proc. Nat. Acad. Sci.U.S.A.* **114**, E5389–E5395 (2017).

20. D. Marjanović, M. Laurin, Phylogeny of Paleozoic limbed vertebrates reassessed through revision and expansion of the largest published relevant data matrix. *PeerJ* **6**, (2019).

21. J. Anderson, R. Reisz, D. Scott, N. Fröbisch, S. Sumida, A stem batrachian from the Early Permian of Texas and the origin of frogs and salamanders. *Nature 2008* **453**, 515–518. (2008).

22. J. H. de Groot, J. L. van Leeuwen, Evidence for an elastic projection mechanism in the chameleon tongue. *P. Roy. Soc. B-Biol. Sci.* **271**, 761–770 (2004).

23. J. L. Van Leeuwen, Why the chameleon has spiral-shaped muscle fibres in its tongue. *Philos. T. Roy. Soc. B* **352**, 573–589 (1997).

24. A. Sakes *et al.*, Shooting mechanisms in nature: a systematic review. *PLOS One* **11**, e0158277 (2016).

25. S. M. Deban, D. B. Wake, G. Roth, Salamander with a ballistic tongue. *Nature* **389**, 27–28 (1997).

26. E. R. Lombard, D. B. Wake, Tongue evolution in the lungless salamanders, family plethodontidae. II. Function and evolutionary diversity. *J. Morphol.* **153**, 39–79 (1977).

27. A. W. Smits, J. I. Flanagin, Bimodal respiration in aquatic and terrestrial apodan amphibians. *Am. Zool.***34**, 247–263 (1994).

28. D. L. Levy, R. Heald, Biological scaling problems and solutions in amphibians. *C. S. H. Perspect. Biol.* **8**, 019166. (2016).

29. F. T. Burbrink *et al.*, Interrogating genomic-scale data for Squamata (lizards, snakes, and amphisbaenians) shows no support for key traditional morphological relationships. *Syst. Biol.* **69**, 502–520 (2019).

30. X. Shen *et al.*, Enlarged multilocus data set provides surprisingly younger time of origin for the Plethodontidae, the largest family of salamanders. *Syst. Biol.* **65**, 66–81 (2016).

Acknowledgments: We are grateful to: Adolf Peretti/Peretti MuseumFoundation for access to their amber collection; Jessica A. Maisano, Matthew Colbert (UTCT | University of Texas) for scans and Anton Maksimenko for technical assistance at the Australian Synchrotron; David Grimaldi (AMNH) for paratype photographs/specimen notes; Stephanie Abramowicz (LACM) for reconstruction of *Yaksha*; and James Gardner and an anonymous reviewer for their important comments to the manuscript. **Funding:** JDD: NSF DEB 1657656, SHSU, ELS: NSF DBI1701714, AB: AB: NF170464 (Royal Society, UK), IJC2018-037685-I and the projectCGL 2017-82654-P, (MICINN, Spain / FEDER, EU) and the CERCA Programme /Generalitat de Catalunya, .AČ: Grant 1/0209/18 (Ministry of Education of Slovak Republic and Slovak Academy of Sciences). **Author contributions:** Project instigated by SEE, JDD and ELS; ELS and JB processed HRCT data; JSA, JDD, and AB performed phylogenetic analyses, with coding input from SEE; AB performed morphospace analyses; paper drafted by SEE with contributions from all authors; Competing interests: The authors declare that they have no competing interests. **Ethics statement:** Specimens were acquired following the ethical guidelines for the use of Burmese amber set forth by the Society for Vertebrate Paleontology (see “Provenance and Ethics” section of the Supplementary Materials for a detailed description of ethical fossil acquisition and accession). We hope this study will serve as a model for other researchers working with these types of materials in this region. **Data and materials availability:** all data available in manuscript or supplementary material; the holotype of *Yaksha Perettii* (GRS-Ref-060829) and refereed specimen are housed at the Peretti Museum Foundation, Switzerland; the

paratype (JZC Bu154) belongs to the James Zigras Collection, housed at the American Museum of Natural History, New York, USA.

Supplementary Materials:

Materials and Methods

Supplementary Text

Figs. S1 to S15

References (*31–69*)

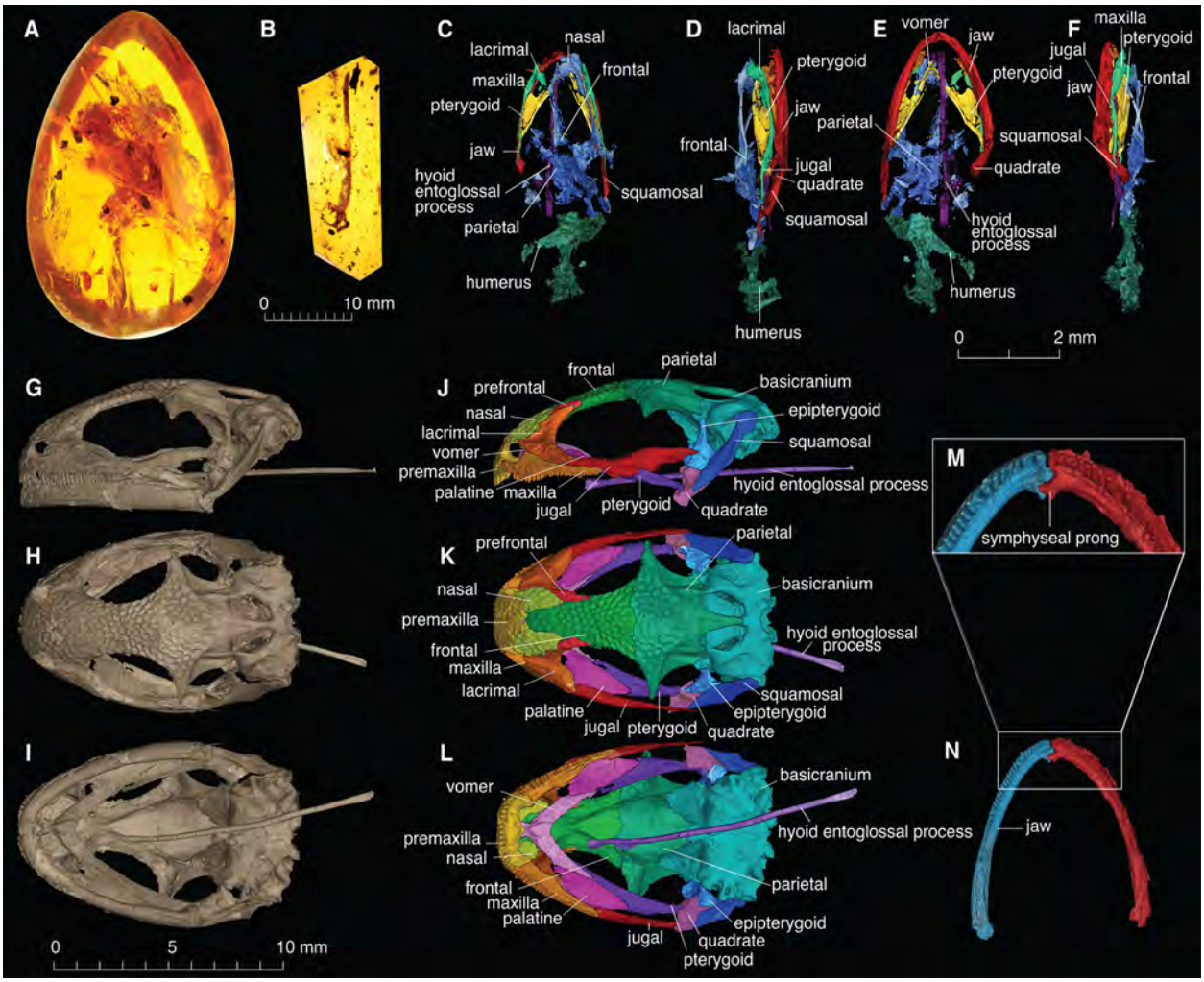

Fig. 1. Holotype and paratype of *Yaksha perettii*. Holotype GRS-Ref-060829 (A, G–I), Paratype JZC Bu154 (B–F), High Resolution Computed Tomography (HRCT) of the paratype with segmented bones (C–F), HRCT of the holotype with jaw articulated (G–I), HRCT of the holotype with all bones segmented and jaw removed (J–L), HRCT of the jaw of the holotype,

with close up of the mandibular symphysis (M–N). Lateral (D, F, G, and J), dorsal (C, H, K, M, and N), ventral (E, I, and L).

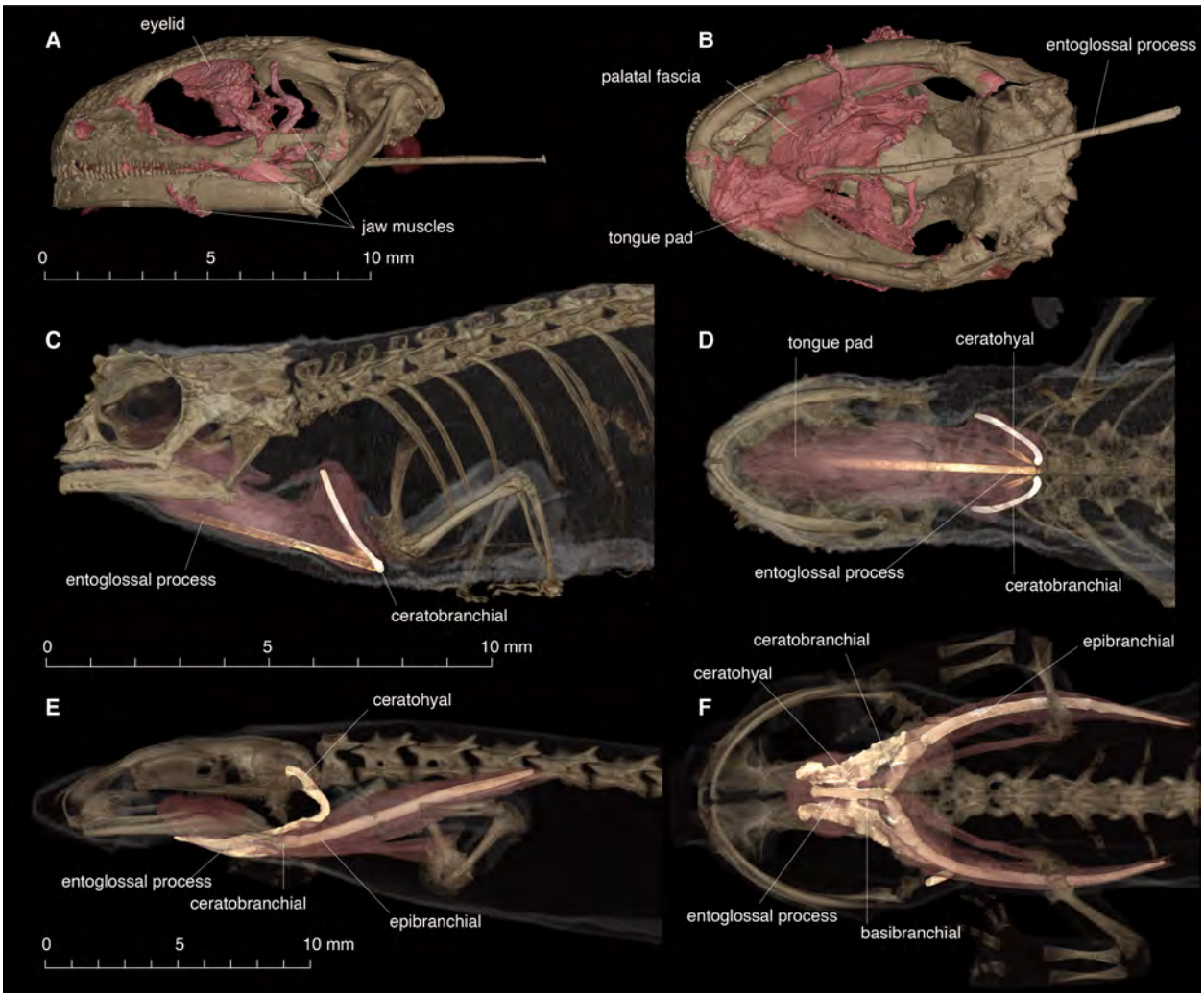

Fig. 2. Comparison of skeletal components in three tetrapods with ballistic tongues. Holotype of *Yaksha perettii* (GRS-Ref-060829) showing the preserved soft tissue (pink), including the tongue in lateral (A) and ventral (B) views; DiceCT – Diffusible Iodine-based Contrast-Enhanced Computer Tomographies of a leaf litter chameleon (*Brookesia* sp. UF

166895) in lateral (C) and ventral (D) views; lungless salamander (*Bolitoglossa porrasorum* UF156522) in lateral (E) and ventral (F) views.

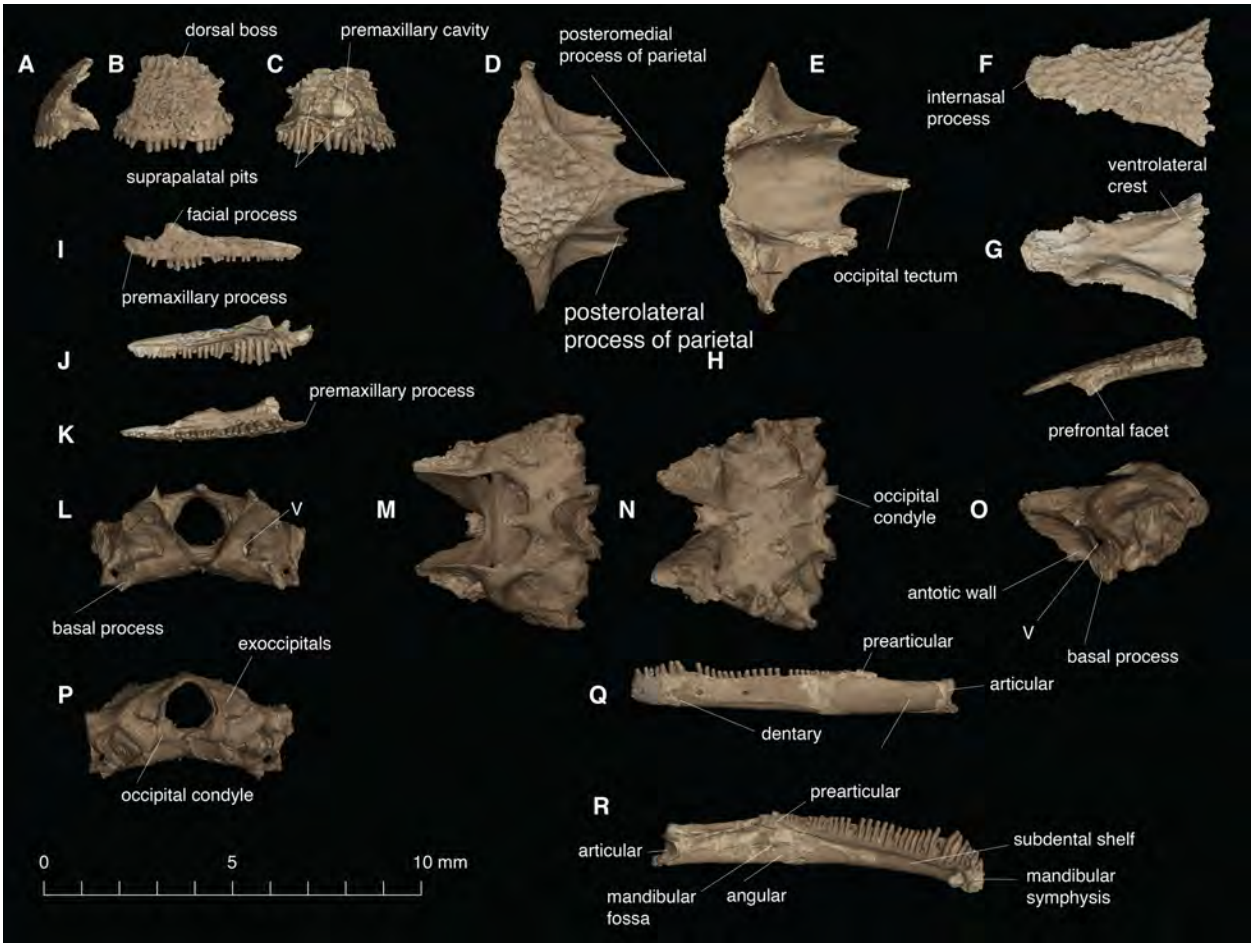

Fig. 3. Isolated elements of the holotype skull of *Yaksha perettii* (GRS-060829). Fused (or tightly paired) premaxillae (A–C), parietal (D–E), frontal (F–H), left maxilla (I–K), basicranium (L–P), left mandible (Q–R). A, H, I, O, Q, lateral view; J, R, medial view; B, L, anterior view; C, P, posterior view, D, F, M, dorsal view; E, G, K, N, ventral view.

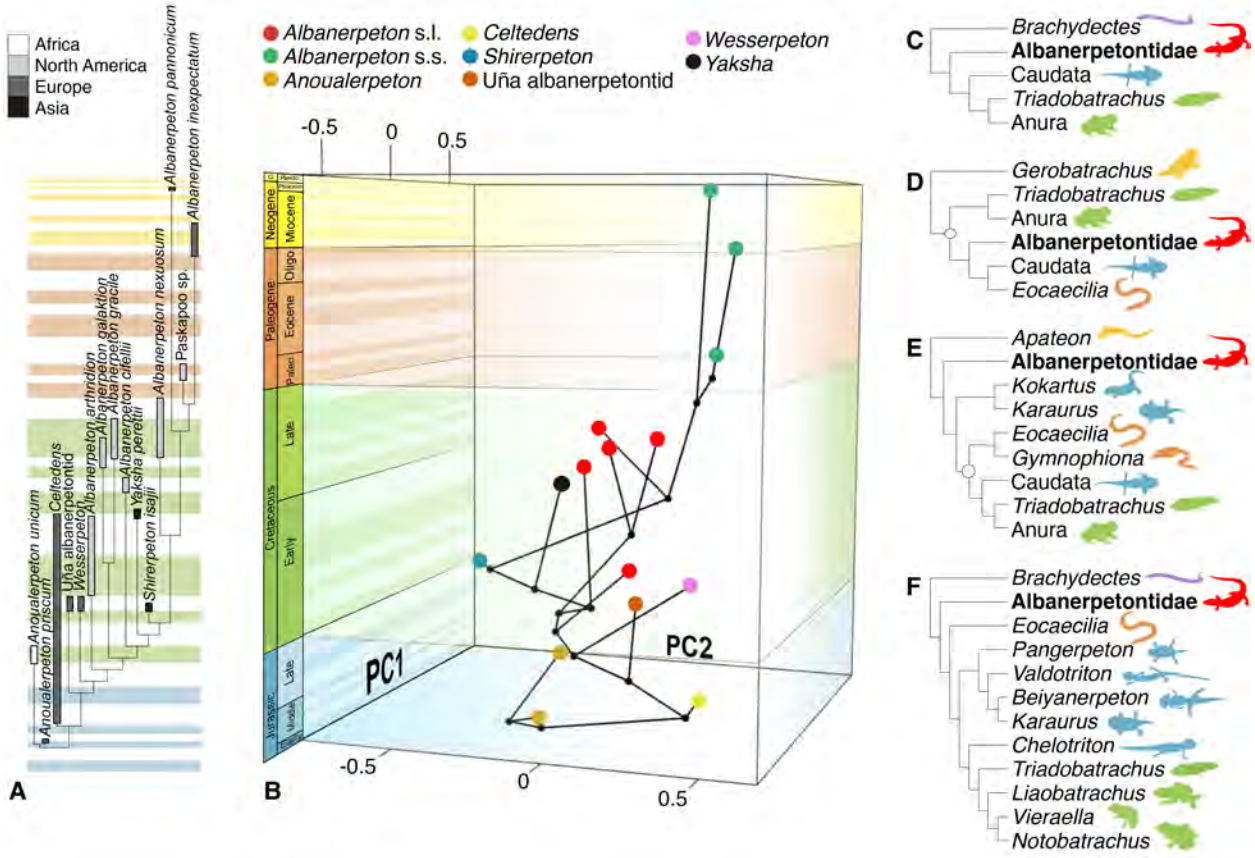

Fig. 4. Phylogenetic relationships of albanerpetontids calibrated against age (A), chronophylomorphospace using the data set for albanerpetontids. PC1 and PC2 explain 35.5% and 23.8% of the total variance (B). Note the position of purported members of the genus *Albanerpeton* in separate clades and regions of the morphospace. The tree was dated using the "equal" method, but we also provide an alternative tree dated under the "mbl" method (Supplementary materials). (C–F) alternative positions recovered for Albanerpetontidae in relation to lissamphibians using different data matrices: C (*22*), D (*23*), E (*24*), and F (*25*).

Science
AAAS

Supplementary Materials for

Enigmatic amphibians in Mid-Cretaceous amber were chameleon-like and had ballistic feeding

Juan D. Daza, Edward L. Stanley, Arnau Bolet, Aaron. M. Bauer, J. Salvador Arias, Andrej Čerňanský, Joseph J. Bevitt, Philip Wagner, Susan E. Evans

Correspondence to: juand.daza@gmail.com

This PDF file includes:

Contents

Figures

S1. Materials and Methods

S1.1 Provenance and Ethical Statement

The holotype of *Yaksha Perettii* (GRS-Ref-060829) and the referred specimen (GRS-Ref-27746) were recovered pre-conflict, in late 2017, by a local commercial miner, using local mining practices at the mining area of Aunbar, in the Hukaung Valley, near Tanaing township, Myitkyina District, Kachin Province, Myanmar. The vertebrate inclusions were discovered during polishing of the amber by Internally Displaced Person (IDP) camp inhabitants, and the specimens purchased by GRS Gemresearch Swisslab (GRS) through an agent, with the profit committed to a charity supporting IDP camps run by the local church. These vertebrate fossils were first presented to one Adolf Peretti by local intermediaries for inspection during a humanitarian mission to the Tanai area, led by GemResearch Swiss Laboratory (GRS).

These specimens were acquired from an authorized company that exports amber pieces legally outside of Myanmar, following an ethical code that assures no violations of human rights were committed in the process of mining, and commercialization. The sample was initially loaned on consignment to GRS during a Bangkok show in 2018, for chemical, physical and spectroscopic analysis. Following these tests, the specimens were returned to Myanmar by the Myanmarese owner, and exported through a jewellery show in Yangon officially through a broker of GRS, whereupon it passed through definitive official export channels, and subsequently entered the GRS collection in Switzerland. AP strongly affirms that no funds from the sale of this amber specimen have been directed to support conflict in Kachin. The movie of the mine visit is available upon request from AP.

Upon completion of scientific measurements, the samples were donated to the Peretti Museum Foundation (PMF), Meggen, Switzerland (https://www.pmf.org/) where they are securely housed. The Peretti Museum Foundation is an officially established, not-for-profit organization, founded in Switzerland by the Peretti family. The PMF actively supports research and collaboration, with all specimens and associated content in the PMF registry accessible to the public onsite, and available on loan for expert collaboration upon written request. The special legal structure of the non-profit “Peretti Museum Foundation” law mandatorily guarantees under Swiss law that inventory of the foundation with GRS Reference numbers can never be lost to science. A description and further details regarding the timing and a discussion of the military escalation in the Tanai area, and details regarding the ethical acquisition of amber pieces from Myanmar are available at the Museum website: https://www.pmf.org. These specimens have also an authenticated paper trail, including

export permits from Myanmar. All documentation is available from the Peretti Museum Foundation upon request. Detail information of the ethical acquisition of amber pieces can be found in the following link: https://bit.ly/2x8gnVj. The paratype was acquired by James Zigras long time before the conflict, as this specimen in a publication from 2016. (*14*). The authors consider they have met the goals laid out in the SVP recommendations.

Myanmar amber specimens containing vertebrate inclusions are extremely rare and generally found only with community effort. The origin of the specimens was verified as being from the Aunbar mining locality by in-house protocols developed by GRS, a gemological research laboratory specializing in the determination of origin and authentication of colored gems. Authenticity and locality were determined by comparison of physical and chemical properties of the specimen (including color, amber flow characteristics, Infrared and UV-fluorescence and photoluminescence spectra, solid micro particle inclusions, fluid inclusion patterns, micro-plant matter debris and accompanying entomological inclusions) against control samples obtained from different mines in the Tannai area, other localities, and against treated and synthetic amber. In total, approximately 4000 amber specimens were included in this analysis, the results of which will be reported in a separate paper. From these tests, GRS-Ref-060829 and GRS-Ref-27746 could not have come from another deposit other than the one indicated by the miners who made the discovery.

The age of the deposit was determined as early Cenomanian, around 99 million years ago (Ma) using U-Pb isotopes (29), and corroborated by analysis of ammonite and insect inclusions found within amber samples sourced from the same locality.

S1.2 CT scanning and segmentation

All specimens were inspected using microCT data. The holotype (GRS-Ref-060829), and referred material (GRS-Ref-27746) were scanned using a NSI scanner with a Fein Focus Microfocal source, at 130 kV and 0.13 mA, and the holotype also scanned using the Imaging and Medical Beamline at the Australian Synchrotron, using 23 keV monochromatic X-rays. The paratype (JZC Bu154) was scanned GE Phoenix vtomex s240 system, with a molybdenum target and modification of the current and voltage to maximize the range of densities recorded. 3D rendering and segmentation were performed using VGStudio MAX version 3.3 (Volume Graphics GmbH).

S1.3 Phylogenetic analyses

Yaksha was retrofitted in a character matrix for albanerpetontids(*7, 16*), comprising16 species and 34 characters. *Yaksha* was also used to complete data scores for Albanerpetontidae in four broader amphibian data matrices (*17-20*) chosen for their taxon sampling but also different views on the lepospondyl vs temnospondyl origin of lissamphibians (Fig. 4, Figs S12-S15). All analyses were performed with TNT (Tree analysis using New Technology) (*31*). We searched for the best tree over all matrices with implied weights (*32-34*), increasing the concavity value using a size of class interval of 10 from 10 to 200. At each run we used a script to search with new technologies (*xmult* command), starting with 20 trees of random addition, using exclusive and random sectorial searches (*35*), as well as 25 rounds of ratchet(*36*) and tree drift(*35*), and fusing trees every five rounds. This procedure was repeated until 20 independent hits of minimal length were found. All the best trees, as well as the strict consensus were stored. A majority rule tree was constructed using all the strict consensus of each concavity value; this tree shows the branches that are stable (i.e. they are optimal under most concavity values).

The plot of phylogeny on a geographical map (Fig. S7) was created using Phytools v. 0.6-99(*37*) in R 3.6.1 (*38*).

S1.4 Morphospace analysis:

Morphospace analyses were run in Claddis package v. 0.2.0 (*39*) in R (Fig. S9). The character data matrix (*7, 16*) was used to calculate a distance matrix that served to plot a morphospace of albanerpetontids in 2D (Fig. S10). The package Plotly v. 4.9.0 (*40*) was used to generate an interactive plot of 3D morphospace (Fig. S11). A most parsimonious tree resulting from the phylogenetic analysis was time calibrated with Paleotree v. 3.3.25 (*41*) and then used to plot a 2D phylomorphospace in ggplot2 v. 3.2.1 (*42*), a 3D phylomorphospace in Geomorph v. 3.2.0 (*43*) and a chronophylomorphospace in Claddis package v. 0.2.0 (*39*).

S2. Supplementary Text

S2.1 Differential diagnosis:

Yaksha perettii resembles the Japanese *Shirerpeton isajii* (*7*) in having a relatively long broad-based frontal internasal process and posteriorly bifurcate parietals that meet the triradiate anterior border of the otic capsule to enclose paired posterior cranial fenestrae, but differs in having slightly shorter, partially sculptured postorbital processes of the parietals (long, unsculptured in *Shirerpeton*), shorter posterolateral processes of the parietals, and a frontal length equal to the maximum parietal anteroposterior length (frontal longer relative to

parietal in *Shirerpeton*). *Yaksha* resembles *Albanerpeton* spp. and *Wesserpeton evansae* (*16*), and differs from *Anoualerpeton* spp. (*8*) and *Celtedens ibericus* (*10*), in having a triangular rather than bell-shaped frontal; differs from all but *Albanerpeton arthridion (3)*, in that the frontal body is short but anteriorly relatively wide, but differs from *Al. arthridion* in having a longer, more pointed frontal internasal process; resembles *Wesserpeton* and *Al. arthridion* in small body size, but differs from both in having a frontal with a longer, more tapered internasal process, an anterior contact between the ventrolateral crests, and in having the posterior margins of the prefrontal facets lying posterior to the frontal mid-length; differs from *Wesserpeton*, *Albanerpeton inexpectatum* (*44*), *C. ibericus*(*10*), and *Anoualerpeton priscum* (*8*), in having parietals with proportionally longer postorbital processes, completely unsculptured dorsally in the lateral half; further differs from *Al. inexpectatum* in lacking fusion of prefrontal and lacrimal, and in having a bifurcate occipital shelf on each parietal. *Yaksha* resembles *Al. inexpectatum* and differs from *Al. pannonicum* (*45*) in exclusion of nasal from narial margin and in showing heterodonty, with distinctly larger anterior dentary teeth. *Yaksha* differs from both Neogene *Albanerpeton* species in the higher dentary tooth number (34-35 vs. 27-29) and the ratio of the anteroposterior frontal length relative to parietal length (frontal shorter relative to parietal in *Al. inexpectatum*). The dentary and maxilla of *Yaksha* resemble *Anoualerpeton* and differ from *Wesserpeton*, *C. ibericus*, unattributed material from the Cretaceous of Uzbekistan ("*Nukusurus*"(*46*)), and *Albanerpeton* (except *Al. nexuosum* (*47*)) in showing size heterodonty and a convex profile of the external alveolar margin.

S2.2 Description of the holotype (GRS-Ref-060829):

The adult skull of *Yaksha perettii* is ovoid in dorsal view, with a blunt rostrum, weakly convex occipital margin, large orbits, and posterior cranial fenestrae. As in all albanerpetontids, the jaw joints lie well anterior to the occipital condyles.

S2.2.1 Skull roof:

- Paired nasals; paired prefrontals; median frontal; paired parietals.
- Characteristic albanerpetontid hexagonal pit and ridge sculpture on all but the lateral and posterior apices of the parietal.

- Ovoid nasals are separated anteriorly by the internasal process of the frontal, contact premaxillae, lacrimals, and prefrontals, but are excluded from the dorsal narial margin by a premaxilla-lacrimal contact.
- The unpaired frontal forms a narrow elongate triangle, with the internasal process forming roughly one third the length of bone. The frontal is weakly embayed anterolaterally by prefrontals, their facets extending well past the midpoint of the frontal (60.6%). At the fronto-parietal suture, the frontal is slightly narrower than in *Shirerpeton* (posterior width/width at posterior edge of prefrontal: 1.84 in *Yaksha* vs 2.08 in *Shirerpeton*). The ventrolateral frontal crests meet in the midline as in *Shirerpeton*, but the contact is further forward, and the crests are more oblique in orientation. There is only a weak mid-ventral crest.
- Like *Shirerpeton*, the paired parietals of *Yaksha* are triangular with a long postorbital process, strongly bifurcated posterior margin, straight median suture, and no parietal foramen. Sculpturing covers the parietal plate except along the lateral and posterior edges, and the fronto-parietal suture is interdigitated. The deep lateral surfaces for external adductor muscle attachment extend into posterolateral processes that contact the prootics. A deep embayment separates the posterolateral process from a longer posteromedial process that, with the contralateral parietal, clasps the anterior ascending process of the occipital tectum (supraoccipital). Ventrally each parietal bears a deep crest, continuous with the ventrolateral crest of the frontal, which separates the concave ventral surface of the postorbital process from the cranial surface. Posteriorly, this crest divides to create a triangular recess for the dorsal edge of the pila antotica ossification.
- The posteriorly embayed parietals create large fenestrae in the roof of the cranial cavity, as in *Shirerpeton* (*7*) but not *Al. inexpectatum*(*44*). These fenestrae are not equivalent to the supratemporal fenestrae of amniotes as they are bounded by the parietal and otic capsules, and open directly into the cranial cavity not the adductor chamber. The sharp edges of the fenestrae suggest they were covered by thick fascia in life. Moreover, neck musculature likely extended across the dorsal surface of this fascia to attach to the unsculptured occipital shelves. The fenestrae may therefore be equivalent to the emarginations that arise, for example, on the scapulocoracoid of lizards, under regions of muscle attachment.

S2.2.2 Circumorbital bones:

- The orbit is framed by the lacrimal, prefrontal, frontal, parietal and jugal; jugal-lacrimal contact excludes the maxilla from the orbital margin. The orbit is confluent with the temporal

fossa posteriorly as there is no jugal-parietal contact. Several foramina perforate the external surface of the lacrimal and open into a single medial foramen for the nasolacrimal duct.

- The curved jugal overlies the dorsal margin of the maxilla anteriorly and its tapered posterior tip almost reaches the squamosal. In *Shirerpeton* (*7*), the jugal was positioned with a posterodorsal orientation, the tip approaching the parietal postorbital process. In *Yaksha* the jugal is more horizontal, but whether this difference is real or a reconstructional error for *Shirerpeton* is uncertain. Tissue traces on the *Yaksha* holotype suggest the orbit was closed posteriorly by soft tissue.

S2.2.3 Upper jaw:

- The premaxilla is the most fully characterised albanerpetontid bone (*3, 8, 45, 48-52*), due to its frequent recovery from microvertebrate deposits and ease of identification. The premaxillae of *Yaksha* are almost rectangular; with a wide unemarginated dorsal process (pars dorsalis). The irregular interpremaxillary suture is most obvious lingually, but the two bones are tightly conjoined and conform to the "robust-snouted" configuration (*51*). The labial surface is divided between an alveolar margin perforated by nutrient foramina, a dorsal process bearing vermiculate sculpturing, and a raised dorsal boss bearing the hexagonal sculpturing found on the skull roof. Lingually, a wide lateral buttress (i.e. internal strut (*56*)), perforated by several small foramina, flanks a medial recess. Gardner (*3, 48, 51*) categorized features of this surface, especially the size and position of the suprapalatal pit. In *Yaksha*, the opening that seems to coincide most closely to the 'pit' in other species is an elongate slot running vertically between the lateral buttress and a second medial strut. A single palatal foramen perforates the palatal plate from dorsal (base of lateral buttress) to ventral (pars palatine). The left premaxilla bears eight tooth positions, the right has ten.
- The maxilla bears a long, broad, dorsally concave premaxillary process forming the entire ventral margin of the naris. The triangular facial process is excluded from the orbital margin by the lacrimal and jugal. Its palatal shelf is embayed anteriorly for the choana, posterior to which it meets the anterolateral margin of the palatine. There are 26 tooth positions.

S2.2.4 Palate:

- The albanerpetontid palate has never been fully described. The choanae are large and obliquely oriented, separated medially by a narrow vomerine bar. There are no distinct

suborbital and subtemporal vacuities, just a narrow cleft between the lateral margins of the palatine and pterygoid and the lower jaw.

- The palatines are large, independent components of the palate. With *Yaksha* for comparison, putative supratemporal of *Shirerpeton* (*7*) can be re-identified as the palatine.
- The pterygoid of *Yaksha* is smaller than the palatine and differs in shape from that of typical frogs and salamanders. The palatal portion meets the posterior ramus of the vomer, excluding the palatine from the interpterygoid vacuity. There is no pterygoid flange and the narrow tapering posterior ramus meets the medial side of the quadrate at its tip.

S2.2.5 Suspensorium and palatoquadrate derivatives:

- The squamosal is long and narrow, with a compressed medial cavity and a tapering ventrolateral margin that support the dorsal and lateral parts of the quadrate respectively. The dorsal head is semicircular and articulates with the paroccipital process of the neurocranium.
- The albanerpetontid palatoquadrate ossifies as two elements – quadrate and epipterygoid. As described for *Shirerpeton*, the quadrate has an anteroposteriorly compressed, ventrally concave, condyle that articulates with the lower jaw. Its dorsal process slots into the recess in the squamosal and it is braced medially by the dorsal flange of the pterygoid. Medially, the quadrate bears a thickened boss. This boss is aligned with the thickened ventral margin of the epipterygoid and the two elements were likely joined by cartilage, the epipterygoid ossifying in the ascending process of the palatoquadrate. Whether the cartilage was continuous or formed a distinct joint is unknown.
- In lateral view, the epipterygoid of *Yaksha* has an expanded base meeting the quadrate and a rod-like dorsal process that contacts the prootic. Seen in anterior view, the epipterygoid bears a thick, curved medial lamina. Its ventral surface meets the quadrate buttress as described above. The ventromedial surface receives the pterygoid, and the dorsomedial surface forms the cranial component of the basicranial joint. Here it is separated from the short basal process (*53, 54*) by a narrow gap that would have been filled in life by cartilage. The epipterygoid, therefore, is the core component linking the suspensorium to the palate.

S2.2.6 Neurocranium:

- The holotype of *Yaksha* preserves a complete and fully articulated neurocranium that is consistent with previous accounts (*7, 44, 53*), but permits a fuller description. It is a complex structure composed of the otic capsules; a median ossification in the tectum synoticum

(supraoccipital) with a long midline process that meets the parietals and separates the dorsal cranial fenestrae; paired exoccipitals perforated by hypoglossal foramina, framing the foramen magnum, and flooring the neurocranium; and a large sphenoid combining a ventral parasphenoid plate, endochondral components forming the basal processes, and large flared anterolateral antotic alae formed by ossification within or adjacent to (perichondrally) the pila antotica of the chondrocranium. There is no basioccipital ossification.

- The conjoined opisthotic and prootic form the otic capsule, the medial margin of which partly frames the cranial fenestra. At its anterior tip, a flange articulates dorsally with the parietal posterolateral process and with the thick pillar supported by the antotic ala, and ventrally with the tip of the epipterygoid. The convex lateral border of the capsule follows the line of the lateral semicircular canal and, at its posterolateral angle, bears a short paroccipital process that articulates with the squamosal.
- The fenestra vestibuli is enclosed by the prootic, opisthotic, and sphenoid. It is large, rounded, and faces posteroventrolaterally. Flat, almost circular bony plates lying within the fenestra are interpreted as stapedes. Anterolateral to the fenestra, the prootic bears a curved ventral crest that meets a bifurcated horizontal crest from the sphenoid to enclose a short vidian canal leading from the back of the skull into the antotic antrum (*55*) (between braincase and epipterygoid). This may have carried the internal carotid artery and/or the jugular vein. Seen in ventral view, however, the bifurcated sphenoid process creates a ventral foramen, for the hyomandibular ramus of the facial nerve.
- The rounded prominence of the anterior semicircular canal separates the otic and antotic regions. The antotic wall is perforated by a small foramen, possibly for the facial nerve. Anteromedial to it, between the otic capsule and the antotic ala, there is a large trigeminal nerve foramen. Ventral to both foramina, the bone is extended into a short, anterolaterally directed basal process. A distinct embayment separates the basal process from the posterior bifurcated prootic process described above, and may have carried the mandibular division of the trigeminal nerve into the adductor chamber. The broad antotic alae flank the central hypophysial fossa and are buttressed by the dorsum sellae. The parasphenoid extends anteriorly for a short distance in the midline but there is no trace of a cultriform process. In a typical fossil skull, this could be interpreted as breakage, but this amber specimen includes remnants of the soft tissues that spanned the interpterygoid vacuity. Had a cultriform process been present, it would have been supported by these tissues, as the underlying hyoid has been. What was previously interpreted as an albanerpetontid parasphenoid rostrum, e.g., (*11*),

was the median hyoid element. In *Shirerpeton*, the antotic alae each support a thickened pyramidal endochondral element that lies dorsally against the skull roof. This was misidentified as a possible epipterygoid (*7*). In *Yaksha*, this endochondral component is more consolidated than in *Shirerpeton*, forming a thick expansion at the dorsal end of the antotic ala that fits a recess in the parietal.

S2.2.7 Mandible:

- The dentary forms the entirety of the lateral surface and supports the ventral angular, biradiate prearticular and terminal articular medially. The conjoined dentaries demonstrate the interlocking structure of the albanerpetontid jaw symphysis, with symphysial prongs fitting into corresponding recesses in the contralateral bone. The movements permitted by this joint (flexion-extension and some rotation) may have aided tongue movements. The concave articular surface for the quadrate is almost vertical.
- The dentary has a sinuous alveolar margin, low at the symphysis, reaching a maximum height (and tooth size) at the level of the premaxillary/maxillary suture, decreasing in height (and tooth size) level with the largest maxillary teeth, and then increasing slightly again towards the back of the tooth row. This is similar to *Shirerpeton*. There are 34-35 tooth positions.

S2.2.8 Hyoid:

- GRS-Ref-060829 preserves the median hyoid element *in situ* as a long cylindrical rod. The anterior end has the greatest diameter, largest central cavity, and thinnest wall. The rod narrows posteriorly, with the wall becoming relatively thicker and the central cavity reducing to a small central core. By analogy with chameleons, the posterior end of the rod would correspond to the basihyal but there is no evidence of articular surfaces for lateral elements (ceratohyal, basibranchial) and neither the adult nor juvenile specimen preserves any trace of other hyoid components. If present, they were cartilaginous. In the juvenile (JZC Bu154), the posterior end of the hyoid rod flattens into a narrow rectangular plate but it is unclear whether this is missing from the end of the adult skull or a taphonomic feature.

S2.2.9 Dentition:

- There is no trace of a zone of weakness within the tooth shaft and therefore no evidence of pedicelly. Labio-lingually bicuspid and pedicellate teeth are considered to be a lissamphibian

character. Pedicellate teeth have also been found in some Dissorophidae (*56*), suggesting that pedicelly, at least at some ontogenetic stage, is the ancestral character of Lissamphibia. However, there is notable heterochronic variation in each of three extant lissamphibian clades as to the transition from non-pedicellate teeth to the stable definitive pedicellate state (*57*). The onset of pedicelly teeth occurs early in the development of Gymnophiona (*58*), whereas in Batrachia (frogs and salamanders), some early stages have non-pedicellate teeth (*57*). If albanerpetontids are related to crown lissamphibians then their non-pedicellate teeth may represent a specialization resulting from heterochrony (*59*).

- The holotype and paratype of *Yaksha* differ in the shape of the tooth crowns. Juvenile teeth are conical with expanded roots and pointed crowns, whereas in the adult, the differences in tooth diameter between the root and the crown are less marked (Figure S2). Such ontogenetic changes in tooth morphology occur in some extant lissamphibians (*60*).
- Both specimens show replacement, with lingually positioned tooth buds and resorption pits at the root of functional teeth. Replacement is most evident in JZC Bu154 (Fig. S2a), where many tooth positions are empty and/or contain the small crowns of replacement teeth. In the holotype (Fig. S2b), fewer tooth positions are undergoing replacement, suggesting that replacement slowed with age. This may explain why evidence of replacement is rare in isolated dentaries from other localities.
- Both the upper and lower jaws of the holotype show heterodonty, with the longest teeth in the midsection of the premaxilla and beneath the facial process of the maxilla. In the lower jaw, the teeth increase in size from the first to the eighth, and then gradually decrease in height along the rest of the row. This results in a sinuous occlusal surface.

S2.2.10 Soft tissue traces:

- GRS-Ref-060829 preserves soft tissue, notably within the orbit, the palate, in association with the median hyoid element, and in the adductor chamber. It confirms that albanerpetontids had scaly eyelids (*10*), supported posteriorly by the postorbital process of the parietal. Ventrally, traces of palatal fascia lie across the interpterygoid vacuity. The anterior part of the tongue is attached to the tip of the median hyoid and there are traces of soft tissue around the hyoid further posteriorly. In the adductor chamber on each side of the head, a rope-like band of tissue extends from the posterior edge of the postorbital process and passes between the pterygoid and jugal to insert on the coronoid process of the mandible. On the right side, a second band of tissue extends from the posterior parietal and inserts on the

mandible anterior to the articular surface. These cranio-mandibular tissue bands are probably remnants of the adductor musculature.

S2.3 Paratype of *Yaksha perettii* (JZC Bu154):

- JZC Bu154 is a tiny (10.6 mm SPL, skull <3.03 mm) juvenile skeleton. It has short limbs with four digits on the manus, and a short, curled tail. The body is not compressed.
- The skull is only partly developed, with the neurocranium largely unossified, and the frontal ossified only along its lateral margins. Ossification has progressed further in the vomer and palatine, as well as the maxillae and mandibles. This pattern is common to many tetrapods whereby dermal bones begin to ossify before cartilage ones, and tend to ossify from ventral to dorsal, and from lateral (orbital margins) to medial. Given the very small size of JZC Bu154 and the incomplete ossification, we interpret it to be very young.
- Daza et al. (*14*) estimated a presacral vertebral count of 15-17 but this was an underestimate. Adult specimens of *C. ibericus* from Spain yielded a count of 22 presacrals (*10*) and, allowing for the scan resolution, JZC Bu154 seems to have roughly the same number. The tail, however, appears surprisingly short compared to the Spanish skeletons. An elongated, vertical scapula blade is preserved on the right side, as in *C. ibericus* (*1*) and, in comparison to chameleons, is a potential adaptation to allow the forelimbs to be brought closer to the midline in climbing (*61*). Parts of forelimb are also preserved on the right side, showing that the hand has four digits, the longest of which is the third. The phalanges appear flattened, but this may be preservational. The elongate unguals are hooked at their tips, a possible adaptation to climbing. The carpus is unossified. In the hind limb, five digits on the foot of which the third and fourth are the longest, and the fourth and fifth are slightly offset from the others. The pedal unguals resemble those of the manus.
- JZC Bu154 preserves epidermal tissues, including weakly discernible scales and well-preserved claw sheaths (Figs. S3-S4). The skin appears partially decayed (covered in parts with a thin, milky film). Most body scales are minute, appearing as small, dark, scattered spots. They are visible under 200X magnification using compound optics with transmitted light (Figs. S3-S4). Larger, less defined, scales are visible on the throat (Fig. S3-S4).
- The specimen lies next to an outstretched millipede (Myriapoda), and the amber piece also contains two more millipedes (Myriapoda: Siphonophoridae); a last-instar planthopper (Hemiptera: Auchenorrhyncha: Fulgoroidea); a pseudoscorpion (Arachnida); a gall midge

(Diptera: Cecidomyiidae); a beetle (Coleoptera indet.); a parasitoid wasp (Hymenoptera: Scelionidae); arthropod fragments; particulate debris; and stellate plant trichomes;

S2.4 Referred material of *Yaksha perettii* (GRS-27746, Fig. S5):

- GRS-Ref-27746 is a partial skeleton consisting of a series of mid-posterior dorsal, sacral, and caudal vertebrae, and the right pelvis (Fig. S4). Vertebral morphology is consistent with that of other albanerpetontids. However, unlike batrachians, GRS-27746 has two sacral vertebrae. This is the first time the sacrum has been preserved clearly in an albanerpetontid.

S3. Systematics

S3.1 Systematic position of *Yaksha* within Albanerpetontidae

We retrofitted *Yaksha* into an existing albanerpetontid matrix(*7,16*) (Character scores in 3.3), and ran an analysis using TNT (*31*). Using either a hypothetical ancestor or *Anoualerpeton* as outgroup, the Majority Rule tree combining the results of all searches (Figs. S6-S12) placed *Yaksha* in an unresolved polytomy with *Shirerpeton*, *Al. nexuosum*, and a clade of Cenozoic albanerpetontids comprising *Al. pannonicum*, *Al. inexpectatum*, and the unnamed Paskapoo sp. (*52*). Another group of species referred to *Albanerpeton* (*Al. cifellii, Al. galaktion, Al. gracile*) formed a polytomy one node stemward, and *A. arthridion*, *Wesserpeton*, the 'Uña albanerpetontid' (*16*), *Celtedens,* and *Anoualerpeton* formed successive outgroups to the main groupings. This is similar to the Strict Consensus tree recovered in the analysis of *Shirerpeton*(*7*). This placement of *Shirerpeton* and *Yaksha* would render *Albanerpeton*, as currently defined, paraphyletic (as noted previously (*7*)).

There are two alternative solutions. The first is to place *Shirerpeton* and *Yaksha* within *Albanerpeton*, maintaining a single genus with a 100 Ma record, from the Early Cretaceous (Barremian) of Asia to the early Pleistocene of Europe (Fig. 4, S8-S9, S12). The second is to restrict the genus *Albanerpeton* to the Cenozoic representatives, namely the Miocene type species *Al. inexpectatum*, the Pliocene *Al. pannonicum*, and the unnamed Paskapoo species, all of which share a distinctive strongly triangular frontal. *Al. arthridion*, *Al. cifellii* + *Al. galaktion* + *Al. gracile*, and *Al. nexuosum* would each be recognized as generically distinct.

The second is our preferred option. The *Yaksha* holotype is the most complete skull of any albanerpetontid. It shares the parietal morphology of *Shirerpeton*, but a few differences (and perhaps also lack of premaxillary data for *Shirerpeton*) mean that the two species are not placed as sister taxa. This situation, where *Albanerpeton* contains several different

morphotypes, is easily visualised if morphospace (resulting from the calculation of a distance matrix of morphological characters) is plotted. (Note: In the tree figured in the main text (Fig. 4), in the biogeographic map (Fig. S7), and in the morphospace analyses (Fig. 4b, S10-S12), we used one of the component trees from the analysis, because for many of the R functions involved, the source tree needs to be fully resolved). All plots (morphospace, 2D phylomorphospace, and 3D phylomorphospace, and chronophylomorphospace, Fig. 4, S8-S9, S12) clearly show a cluster formed by the three Cenozoic species that could be considered as *Albanerpeton sensu stricto. Al. nexuosum* is closest to this clade, mainly in the 3D phylomorphospace (most reliable as a greater variance is included). *Shirerpeton* and *Yaksha* would occupy an intermediate position between this clade and a paraphyletic assemblage comprising the remaining North American taxa currently assigned to *Albanerpeton*. Finally, the European Mesozoic taxa cluster together, with *Wesserpeton* closest to the North American group, and *Celtedens* and *Anoualerpeton* in more stemward positions.

We have, therefore, given separate generic and specific status to the Myanmar form, reflecting the morphological differences, but also those of time and biogeography (Fig. S7). Revising the taxonomy of the Cretaceous species currently referred to *Albanerpeton* is beyond the scope of the present article. It requires a careful re-assessment of the current diagnoses of these taxa, analysis of inter- and intraspecific variation in premaxillary characters, and identification of further elements from microvertebrate deposits.

Most records of albanerpetontids stem from northern (Laurasian) continental landmasses. There are two exceptions, both from Morocco (*8, 9*), but they occur in association with a primarily Laurasian fauna and were likely immigrants. However, there is a growing consensus, based on geology, flora, and invertebrate faunas, that what is now northwestern Myanmar was an island landmass in the mid-Cretaceous, with southern (Gondwanan) origins (*62*). If so, *Yaksha* represents either a lineage that rafted from Asia, which lay to the north (small size, life-style, and possible direct development would have aided this), or a previously unknown southern distribution for the group.

S3.2 Systematic position of Albanerpetontidae within Tetrapoda

In many recent analyses, Albanerpetontidae was grouped with Lissamphibia (Anura, Urodela, and Gymnophiona), but variably placed: as caudates or stem-caudates (*17, 21, 63, 64*); as stem-batrachians (*1, 10, 52,65-66*); as the sister group of Gymnophionomorpha (*18, 67, 68*); or as stem-lissamphibians (53, *64, 68*) . With lissamphibians, albanerpetontids share a bicotylar atlanto-occipital joint, a four digit manus, ectochordal vertebrae with cylindrical

centra, ribs that do not encircle the body, and a salamander-like quadrate-squamosal articulation. Albanerpetontids differ from extant lissamphibians in their keratinized claw sheaths (extant clawed frogs, *Xenopus laevis*, [and possibly *Onychodactylus* within salamanders], share non-homologous claw sheath growth with amniotes (*69*)), their retention of several skull elements including epipterygoids, supraoccipitals, and large palatine bones, and the absence of either tooth pedicelly or a wide parasphenoid cultriform process. If Lissamphibia is monophyletic and albanerpetontids lie on, or close to, the lissamphibian stem, they have the potential to shed light on the ancestral morphology (and therefore origins) of the crown clade. To re-explore the relationships of albanerpetontids to other clades, we coded *Yaksha* into four recent extensive matrices for tetrapods (*17*-*20*). These matrices took source material from Anderson et al. (*21*) and Maddin et al. (*64*). In all cases, data from *Yaksh*a enhanced the existing data on albanerpetontids and changed some character scores.

a) **Huttenlocker et al. (*17*). (**Fig. 4, S13). Albanerpetontidae were placed as the sister group of Salientia (frogs) and Caudata (salamanders) within brachydectid lepospondyls. *Eocaecilia* was placed as the sister taxon to *Rhynchonkos* within microsaur lepospondyls.
b) **Pardo et al. (*18*).** (Fig. 4, S14**).** Albanerpetontids were placed as the sister taxon to *Eocaecilia* and Caudata, with Salientia as the sister group to that clade. This monophyletic Lissamphibia grouped with amphibamid temnospondyls.
c) **Pardo et al. (*19*).** (Fig. 4, S15). This matrix contains a wider sampling of lissamphibian taxa and yielded a more traditional topology with Anura and Caudata as sister taxa, and Gymnophiona as the sister group of these. However, it places two fossil ‘caudate’ taxa (*Karaurus, Kokartus*) on the stem of Lissamphibia (rather than within Caudata), and places Albanerpetontidae as the sister to this more inclusive clade. As in Pardo et al. (*24*), lissamphibians fall within amphibamid temnospondyls.
d) **Marjanovic & Laurin (*20*).** (Fig. 4, S16). When the matrix was run unordered, a monophyletic Lissamphibia (Gymnophiona [Salientia+Caudata]) was nested within aistopod lepospondyls with albanerpetontids placed with lepospondyl microsaurs. With the characters ordered, both Lissamphibia and Albanerpetontidae are placed within Microsauria, although albanerpetontids and a *Batropetes*+*Quasicaecilia*+*Carrolla* clade lie in an unresolved trichotomy with Lissamphibia.

In summary, therefore, there remains no consensus as to the position of lissamphibians in relation to either lepospondyls or temnospondyls, nor to the position of albanerpetontids in relation to individual groups of Lissamphibia. One major problem continues to be the dearth

of early lissamphibian fossils and the temporal gap between putative ancestors (lepospondyl or temnospondyl) and the earliest protofrogs and stem caudates.

3.3 Character scores

Huttenlocker et al. (*17*).

Albanerpetontidae 32011????? 00002101?? 110001000[01] 011100110? ???01???1? 0??1???11? ??01000010 011[01][01]1[01]110 121010311? 001?101001 11?11002?1 001111001? ?0?00202?1 10?2?3??11 00?01??120 0010201001 0010001122 2201020020 1?3??????? ??1??10011 1001000110 2?1000110? 00??100

Pardo et al. (*18*).

Albanerpetontidae 1000--0000 000000000? 0101011110 001---0010 0-0001---- 1-----0100 ---?-?-0-1 ---?21000- -0010-11-1 0-001?0010 000?1001?1 100--0000- 0100-00?00 -0-0010-00 –00001100 02-???-100 00----0002 10-----??? ???????01? 2112011000 111?10100- ?03201--01 111100[01]101 --0-2--110 1[01]11210010 111-111100 1202-11-2- 3--010?120 01010[01]1102 221100?310 010100001- 0000113011 0-0-?10--- ?--120000- 0---00

Pardo et al. (*19*).

Albanerpetontidae 32021???00 01101??110 0010000011 0011?????0 1???1?21?? ?11????1000 10001001[01]1 101310000? 11300?0120 2?110?2?31 100??1??12 000102010? 1001000110 222?112002 01?2?????? ???1??1001 1001000110 2?1000110? ?100??1011 ?20?0?1?01 0002021111 001112101? 201?001?10 0000102011 ?100001??1 ?010012?1? 1010012111 10110101?1 011012301? 1100?0???? ?10?001?1? 10????????0 0?????????0 1011???220 21102??100 0??1110??? 0?1?31010

Marjanovic & Laurin (*20*).

Albanerpetontidae 20201111[01]1 1010001001 1000202101 --11100-2- 0-0-1----- --10--1--1 -------001 0101001--- 1002222002 1-03101?14 0210201101 01103---00 000-011000 02141-01-1 0211[12]31--- 2000--1--0 -11---1--- 1---1----- 00000000[12][12] ---?????1? 0?1?010111? ?11211112? 110?00???? 00?2?00??0 0110000001 1?10011?11 1010200?2 -?00031

References (*31–69*):

31. P. Goloboff, S. A. Catalano, TNT version 1.5, including a full implementation of phylogenetic morphometrics. *Cladistics* **32**, 221–238. (2016).
32. P. A. Goloboff, Estimating character weights during tree search. *Cladistics* **9**, 83–91 (1993).
33. P. A. Goloboff, A. Torres, J. S. Arias, Weighted parsimony outperforms other methods of phylogenetic inference under models appropriate for morphology. *Cladistics* **34**, 407–437 (2018).
34. P. A. Goloboff, J. M. Carpenter, J. S. Arias, D. R. Mirande-Esquivel, Weighting against homoplasy improves phylogenetic analysis of morphological data sets. *Cladistics* **24**, 758–773 (2008).
35. P. A. Goloboff, Analyzing large data sets in reasonable times: solutions for composite optima. *Cladistics* **15**, 415–428 (1999).
36. K. C. Nixon, The parsimony ratchet, a new method for rapid parsimony analysis. *Cladistics* **15**, 407–414 (1999).
37. L. J. Revell, phytools: An R package for phylogenetic comparative biology (and other things). *Methods Ecol. Evol.* **3**, 217–223 (2012).
38. R Core Team. (R Foundation for Statistical Computing, Vienna, Austria., 2013).
39. G. Lloyd, Estimating morphological diversity and tempo with discrete character-taxon matrices: implementation, challenges, progress, and future directions. *Biol. J. Linn. Soc.* **118**, 131–151 (2016).
40. C. Sievert, Plotly for R. (2018).
41. D. W. Bapst, P. J. Wagner, Paleontological and Phylogenetic Analyses of Evolution, Package ‘paleotree’, v. 3.3.25. (2019).
42. H. Wickham *et al.*, ggplot2: Create Elegant Data Visualisations Using the Grammar of Graphics, v 3.2.1. (2019).
43. D. Adams, M. Collyer, A. Kaliontzopoulou, Geomorph: Geometric Morphometric Analyses of 2D/3D Landmark Data, v. 3.2.1. (2020).
44. R. Estes, R. Hoffstetter, Les urodèles du Miocène de La Grive-Saint-Alban (Isère, France). *Bull. Mus. Nat. Hist. Nat., Sci. Terre* **57**, 297–343. (1976).
45. M. Venczel, J. D. Gardner, The geologically youngest albanerpetontid amphibian, from the Lower Pliocene of Hungary. *Palaeontology* **48**, 1273–1300 (2005).
46. L. Nesov, Cretaceous salamanders and frogs of Kizylkum Desert (in Russian). *Proc. Zool. Inst., Acad. Sci. USSR* **101**, 57–88 (1981).

47. R. Estes, Systematics and paleogeography of some fossil salamanders and frogs. *Nat. Geograph. Soc. Res. Rep.* **14**, 191–210 (1982).

48. J. D. Gardner, New albanerpetontid amphibians from the Albian to Coniacian of Utah, USA - Bridging the gap. *J. Vert. Paleontol.* **19**, 632–638 (1999).

49. J. D. Gardner, Revised taxonomy of albanerpetontid amphibians. *Acta Palaeontol. Pol.* **45**, 55–70 (2000).

50. J. D. Gardner, Comments on the anterior region of the skull in the Albanerpetontidae (Temnospondyli; Lissamphibia). *Neues Jahrb. Geol. P-M.* **2000**, 1–14 (2000).

51. J. Gardner, Albanerpetontid amphibians from the Upper Cretaceous (Campanian and Maastrichtian) of North America. *Geodiversitas* **22**, 349–388 (2000).

52. J. D. Gardner, Monophyly and intra-generic relationships of *Albanerpeton* (Lissamphibia; Albanerpetontidae). *J. Vert. Paleontol.* **22**, 12–22 (2002).

53 H. C. Maddin, M. Venczel, J. D. Gardner, J. C. Rage, Micro-computed tomography study of a three-dimensionally preserved neurocranium of *Albanerpeton* (Lissamphibia, Albanerpetontidae) from the Pliocene of Hungary. *J. Vert. Paleontol.* **33**, 568–587 (2013).

54. C. S. Rose, in *In Amphibian Biology. Volume 5. Osteology.,* H. Heatwole, M. Davies, Eds. (Chipping Norton: Surrey Beatty & Sons, 2003), pp. 1684–1781.

55. E. Francis, *The Anatomy of the Salamander*. (Oxford University Press, London, 1934).

56. J. R. Bolt, Dissorophoid relationships and ontogeny, and the origin of the Lissamphibia. *J. Paleontol.* **51**, 235–249 (1977).

57 A. B. Vassilieva, S. V. Smirnov, Development and morphology of the dentition in the Asian salamander, *Ranodon sibiricus* (Urodela: Hynobiidae). *Russ. J. Herpetol.* **8**, 105–116 (2001).

58. M. H. Wake, Fetal tooth development and adult replacement in *Dermophis mexicanus* (Amphibia: Gymnophiona): field versus clones. *J. Morphol.* **166**, 203–216 (1980).

59. J. Gardner, Monophyly and the affinities of albanerpetontid amphibians (Temnospondyli; Lissamphibia). *Zool. J. Linn. Soc.* **131**, 309–352 (2001).

60. T. Davit-Béal, H. Chisaka, S. Delgado, J. Y. Sire, Amphibian teeth: current knowledge, unanswered questions, and some directions for future research. *Biol. Rev.* **82**, 49–81 (2007).

61. J.-P. Gasc, Adaptation à la march arboricole chez le cameleon. *Arch. Anat. Histol. Embryol. Norm. Expériment.* **46**, 81–115 (1963).

62. G. Poinar, Burmese amber: evidence of Gondwanan origin and Cretaceous dispersion. *Hist. Biol.* **31**, 1304–1309 (2019).

63. L. Trueb, R. Cloutier, in *Origins of the higher groups of tetrapods: controversy and consensus.,* H.-P. Schultze, L. Trueb, Eds. (Cornell University Press, Ithaca, 1991), pp. 223–313.

64. H. Maddin, F. J. Jenkins, J. Anderson, The braincase of *Eocaecilia micropodia* (Lissamphibia, Gymnophiona) and the origin of caecilians. *PLOS One* **7**, e50743. (2012).

65. M. Ruta, J. Jeffery, M. Coates, A supertree of early tetrapods. *Proc. R. Soc. Lond. B. Biol Sci* **270**, 2507–2516 (2003).

66. E. Ascarrunz, J. Rage, P. Legreneur, M. Laurin, *Triadobatrachus massinoti,* the earliest known lissamphibian (Vertebrata: Tetrapoda) re-examined by μCT scan, and the evolution of trunk length in batrachians. *Contrib. Zool.* **85**, 201–234. (2016).

67. M. Ruta, M. I. Coates, Dates, nodes and character conflict: addressing the lissamphibian origin problem. *J. Syst. Palaeontol.* **5**, 69–122 (2007).

68. D. Marjanović, M. Laurin, A re-evaluation of the evidence supporting an unorthodox hypothesis on the origin of extant amphibians. *Contr. Zool.* **77**, 149–199 (2008).

69. H. Maddin, S. Musat-Marcu, R. Reisz, Histological microstructure of the claws of the African clawed frog, *Xenopus laevis* (Anura: Pipidae): implications for the evolution of claws in tetrapods. *J. Exp. Zool. B. Mol. Dev. Evol.* **308**, 259–268 (2007).

Fig. S1. Ballistic tongue representation of *Yaksha perettii*. The albanerpetontid is dwelling in the understory of the forest (comparable to Madagascan leaf litter chameleons, which climb in between leaves, twigs and pieces of bark), and is illustrated an instant before being trapped by tree resin. The setting is based on other inclusions in the amber pieces containing the holotype and paratypes (e.g. millipede, pseudoscorpion), and on morphological data from the fossils described. Scientific illustration by Stephanie Abramowicz.

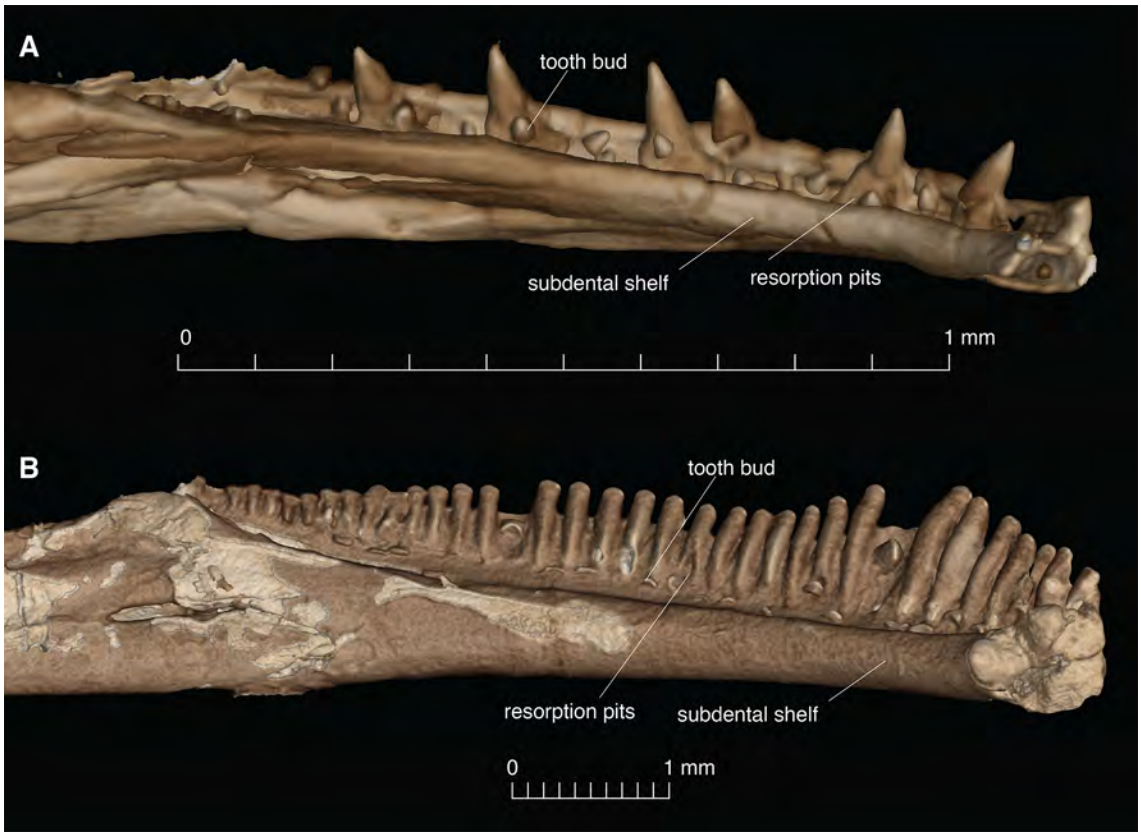

Fig. S2. Lingual views of the right lower jaw. The juvenile paratype (JZC Bu154) (A), and the adult holotype (GRS-060829) (B), to show tooth replacement and the positioning of the replacement tooth crowns in the gaps left by eroded mature teeth.

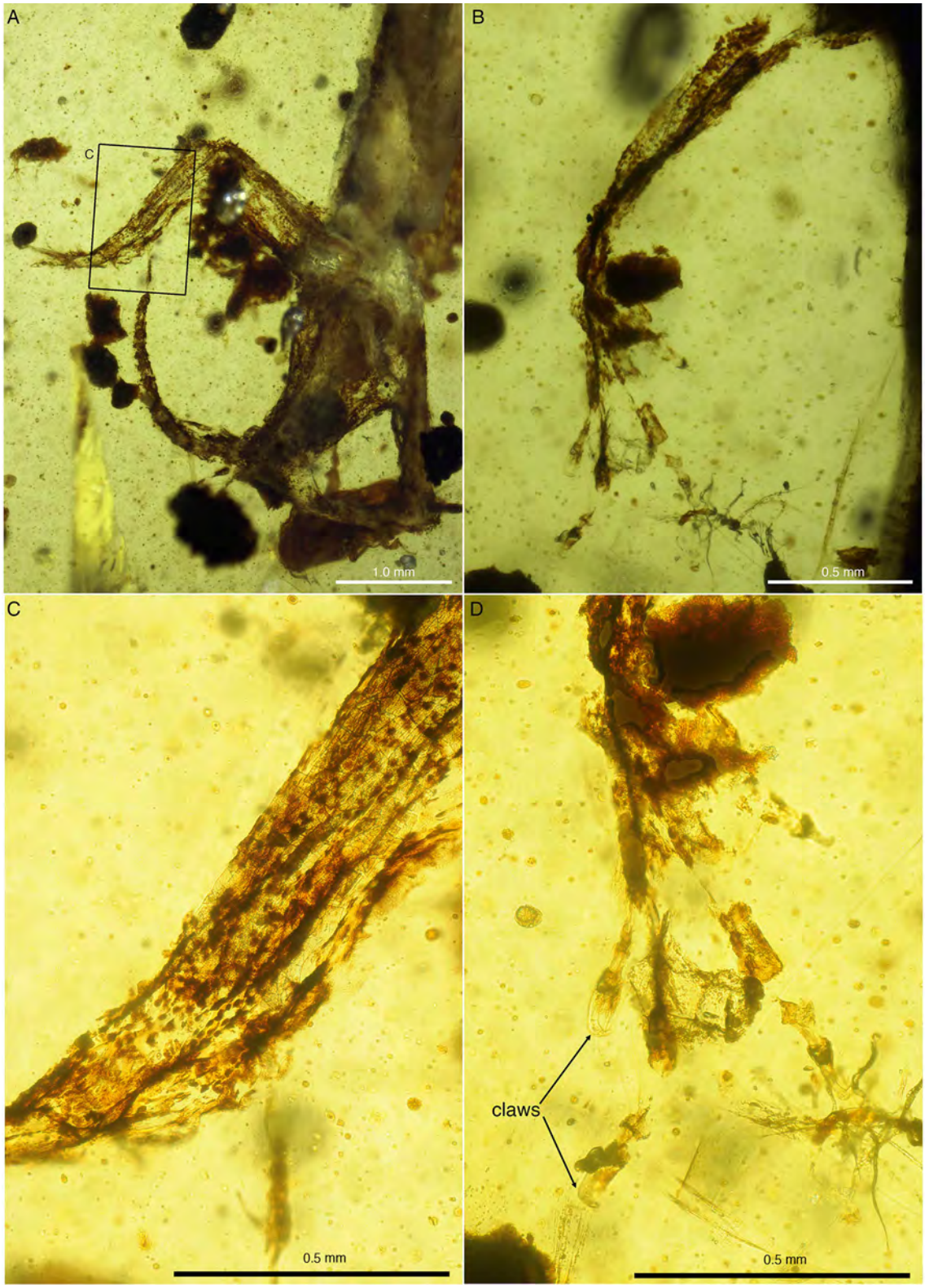

Fig. S3. Details of the paratype of *Yaksha perettii* (JZC Bu154). Dorsal view of the posterior limbs lower back, pelvic, caudal regions (A), left anterior limb (B), close up of the leg showing scales (C), and details of the keratinized claw sheaths in the left anterior limb (D).

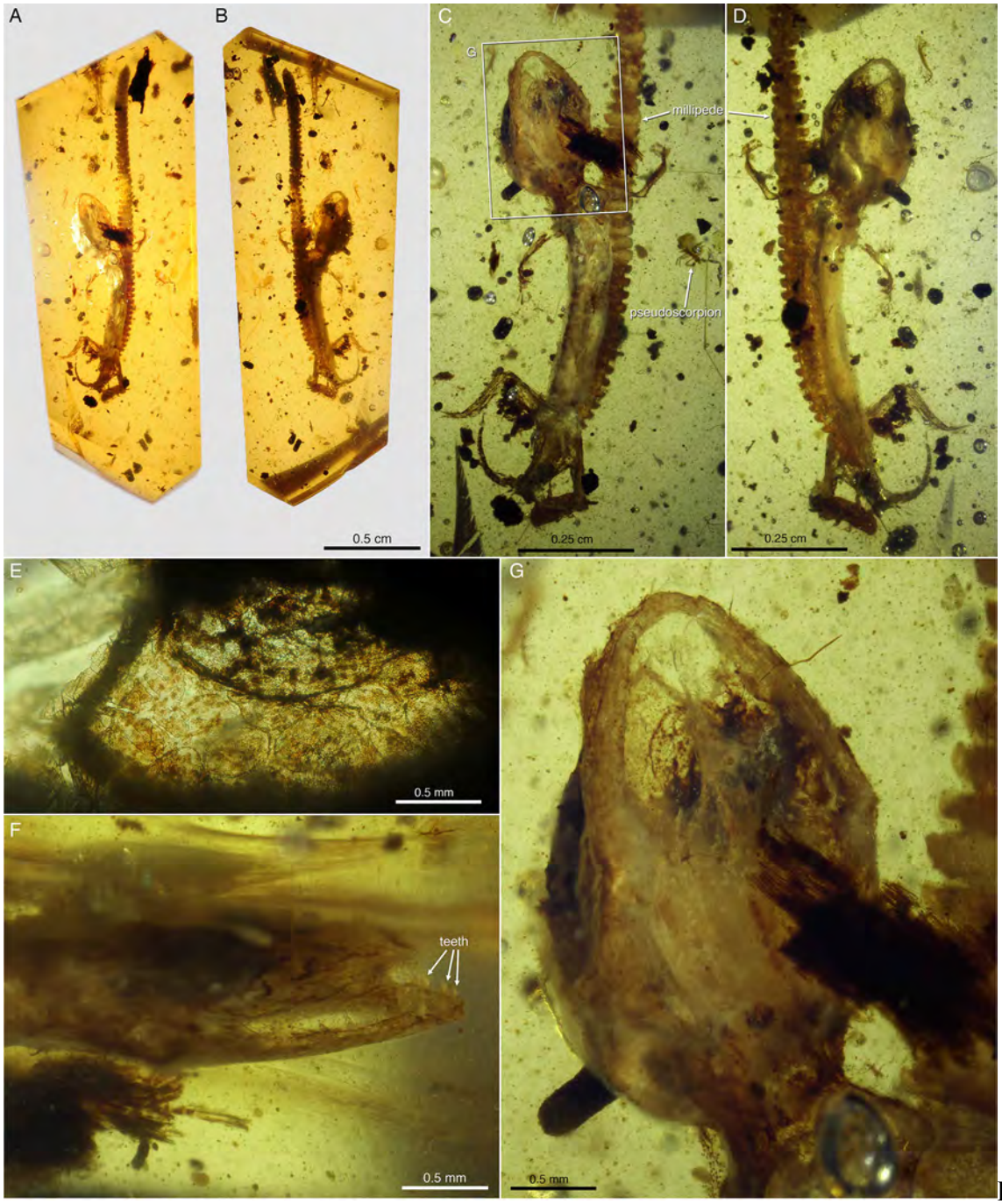

Fig. S4. Details of the paratype of *Yaksha perettii* (JZC Bu154). Whole specimen in ventral (A, C) and dorsal views (B, D) with associated material. Details of small scales covering the body (E), teeth (F) and head in ventral view (G).

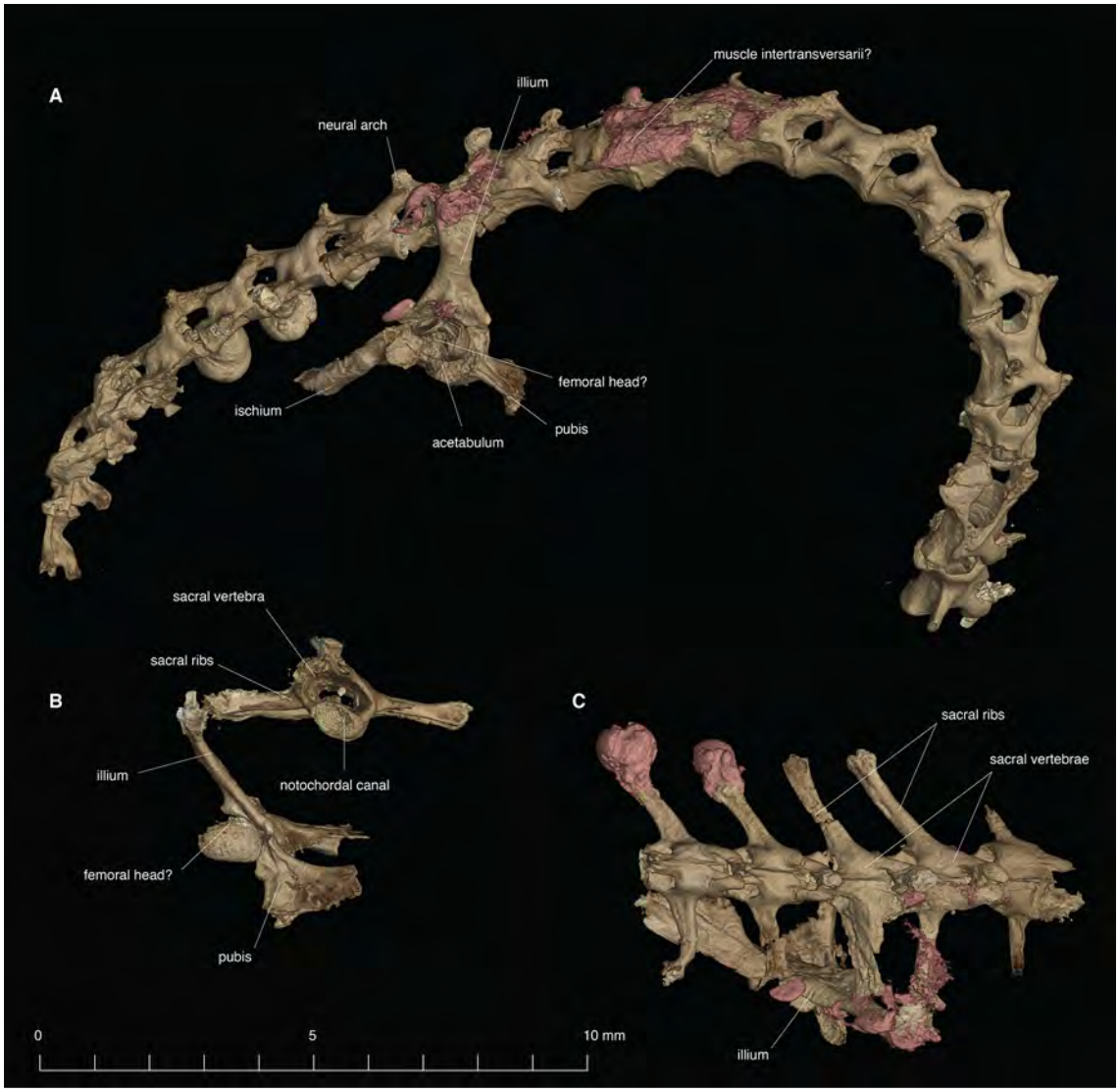

Fig. S5. Postcranium referred to *Yaksha perettii* (GRS-27746). Right lateral view of pelvic elements, presacral, sacral, and caudal vertebrae (A), anterior view of the sacral vertebrae and pelvic elements (B), dorsal view of the sacral vertebrae (C).

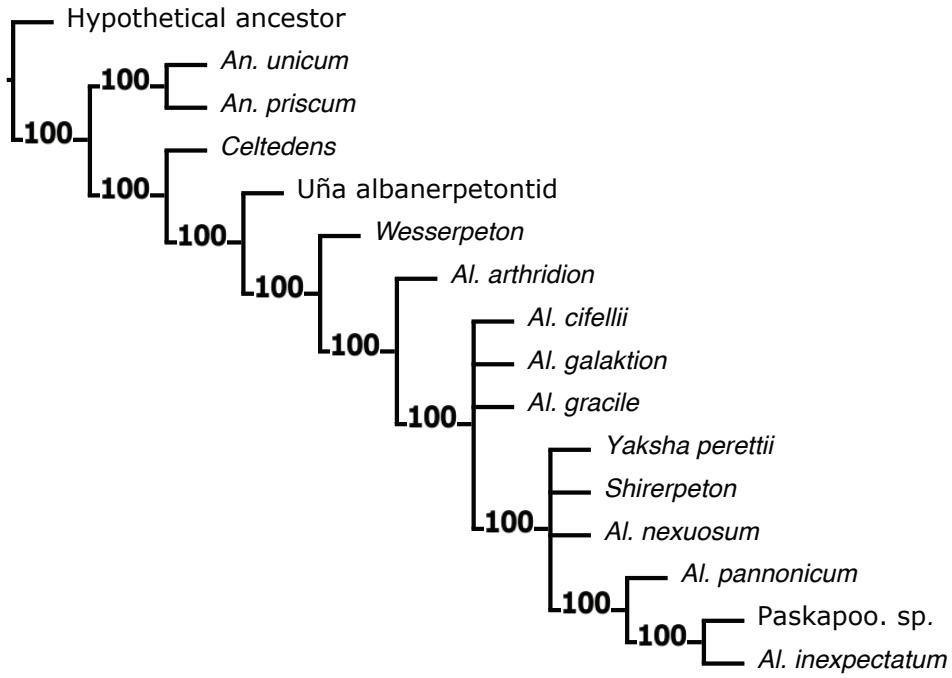

Fig. S6. Results of adding *Yaksha* to the albanerpetontid data set (*7, 16*). Results of searches using implied weights, increasing the concavity value using a size of class interval of 10 from 10 to 200. The tree is the majority rule representing all searches. Values on nodes indicate the percentage of that node being recovered when considering all analyses.

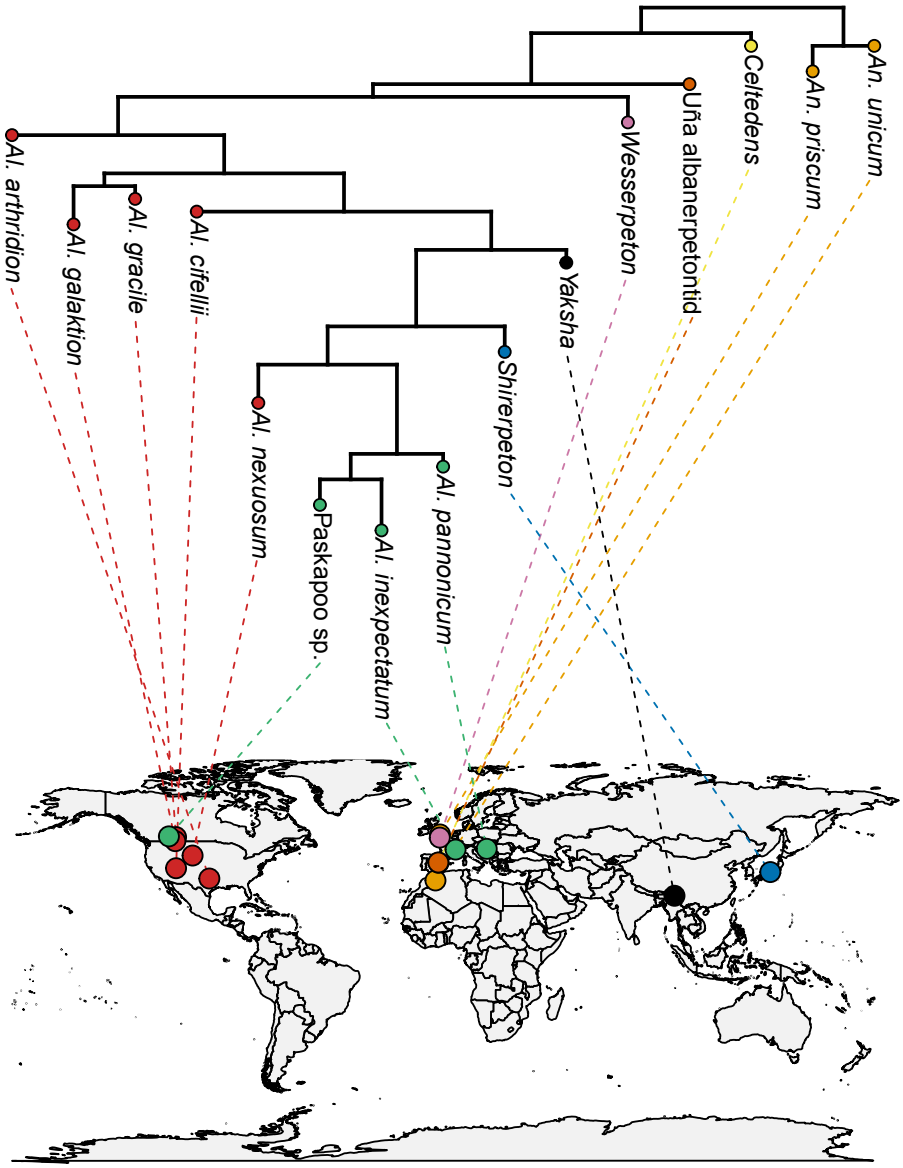

Fig. S7. Geographical distribution of the type specimens (or the main record in the case of the two forms not formally referred to a specific albanerpetontid) and corresponding phylogeny.

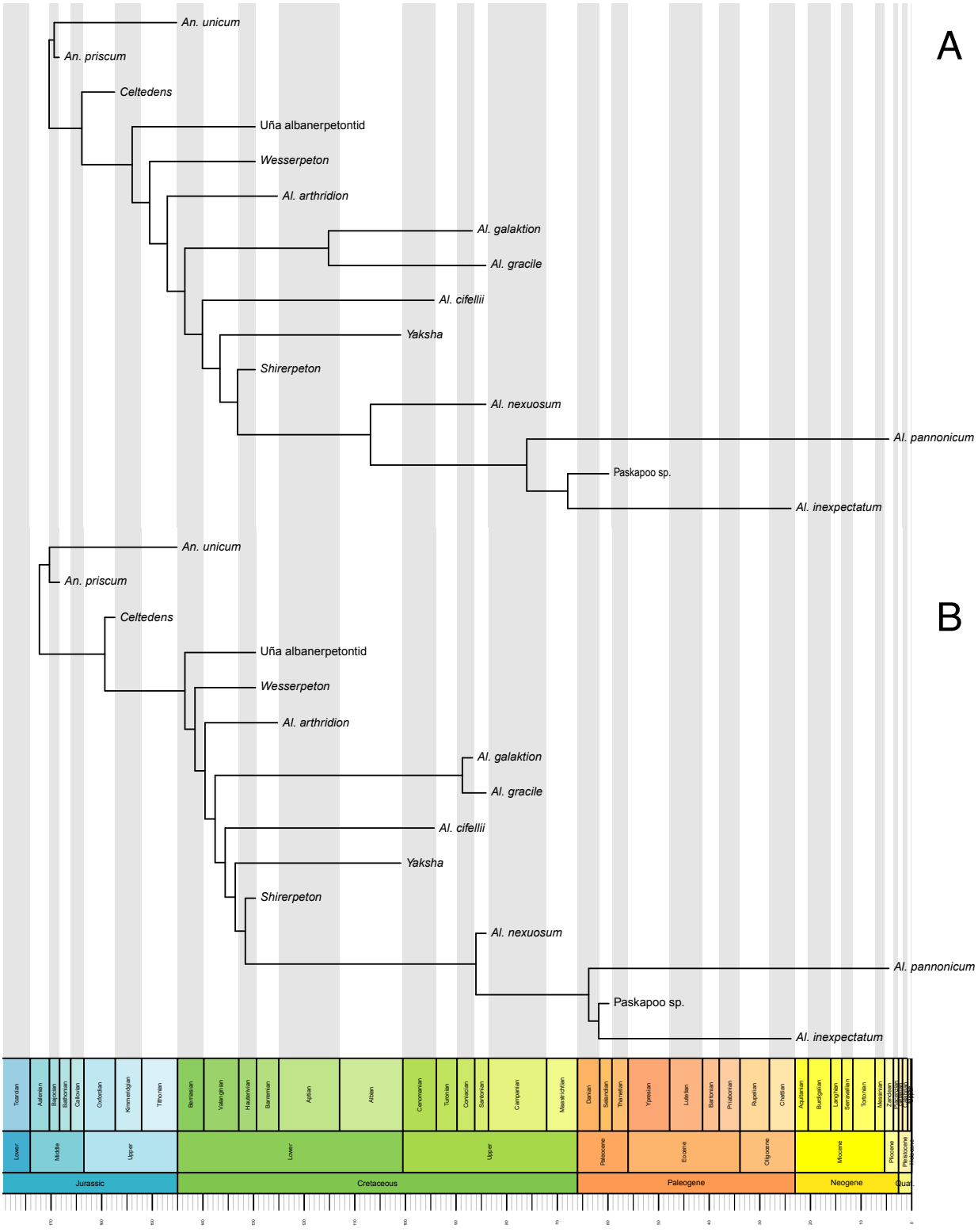

Fig. S8. Temporally calibrated phylogeny under the "equal" method (A), and temporally calibrated phylogeny under the "mbl" method (B). The "equal" method increases the time of the root divergence by some amount and then adjusts zero-length branches so that time on early

branches is reapportioned out along those later branches equally. The “mbl” method rescales a tree with edge lengths so that all edge lengths are at least some minimum branch length (in this case 2 myrs) (*41*).

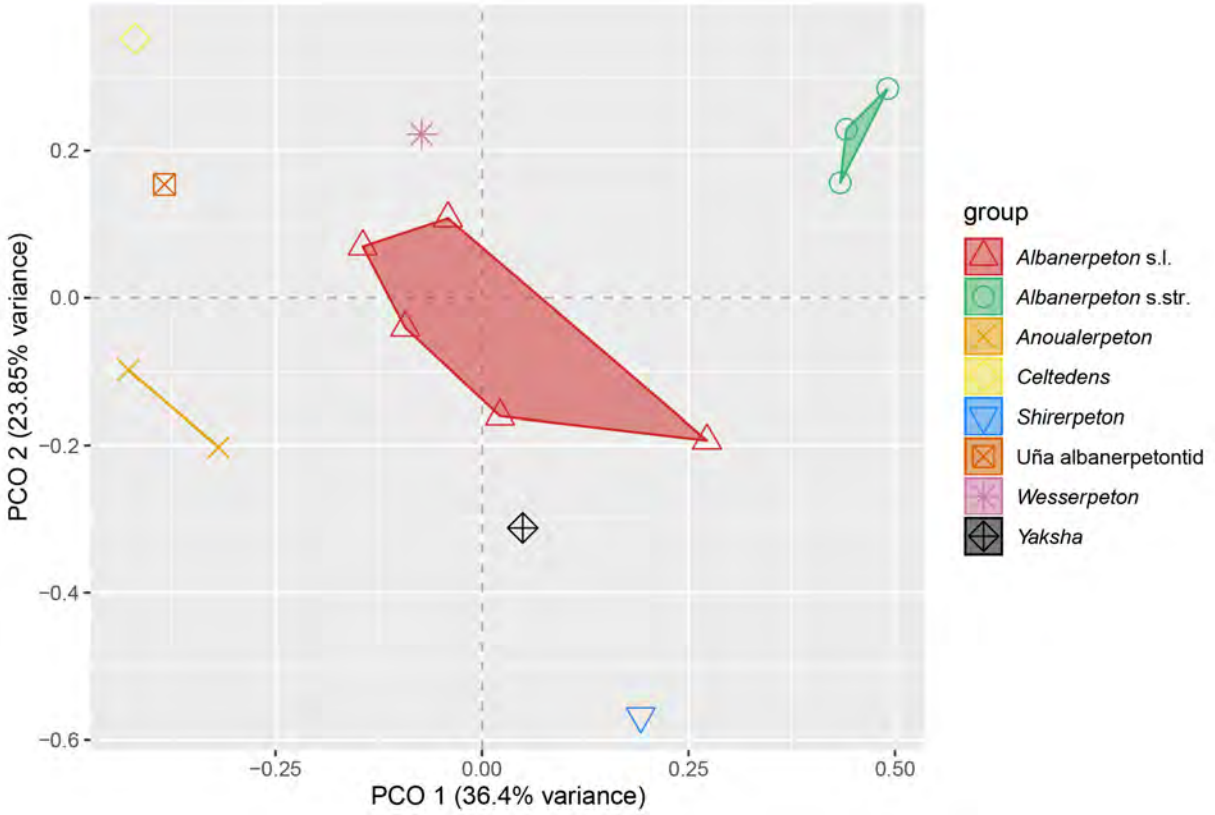

Fig. S9. Morphospace for the matrix of albanerpetontids. Colors and symbols correspond to taxonomic groups. The graph shows the separation between *Albanerpeton* s.l. and *Albanerpeton* s.str.

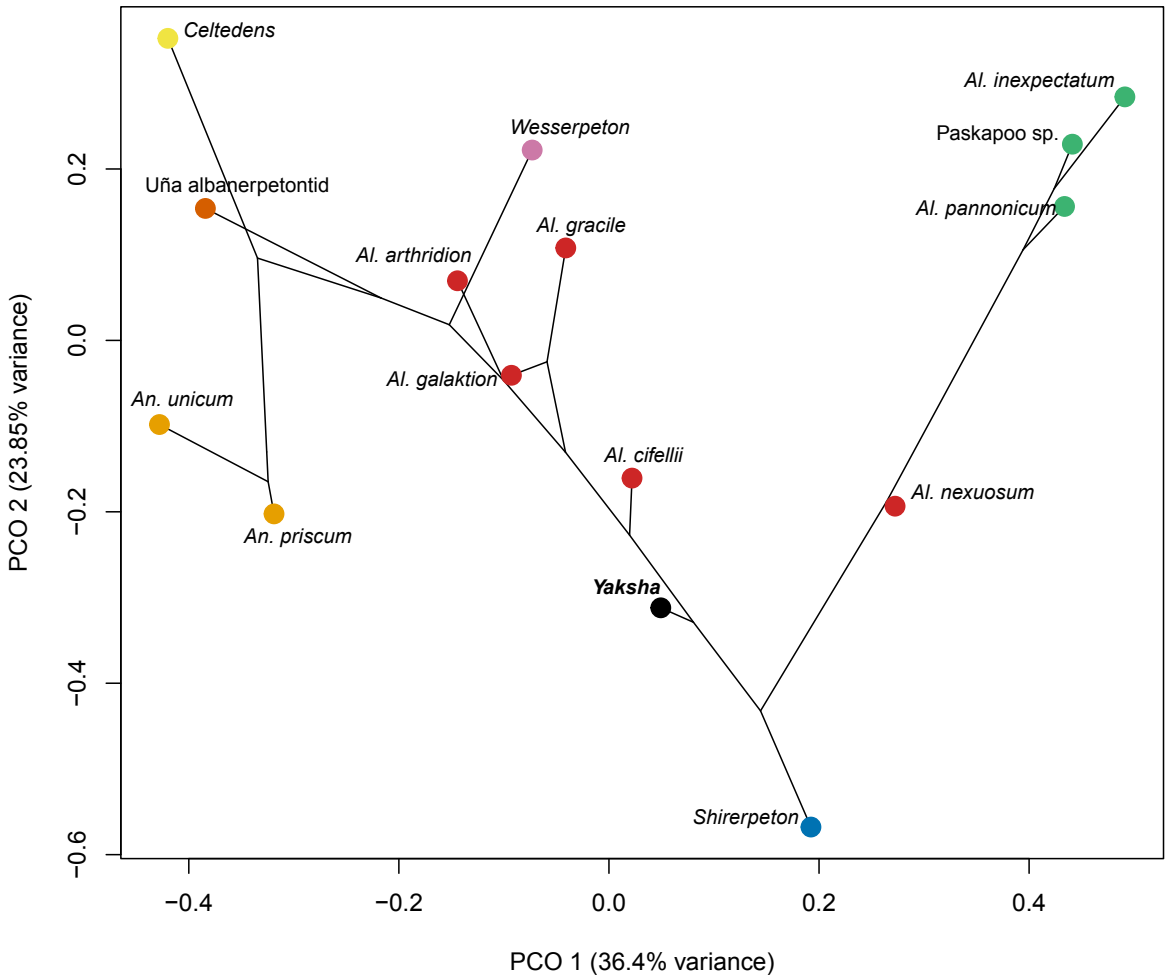

Fig. S10. 2D phylomorphospace for the matrix of albanerpetontids. Colors correspond to taxonomic groups.

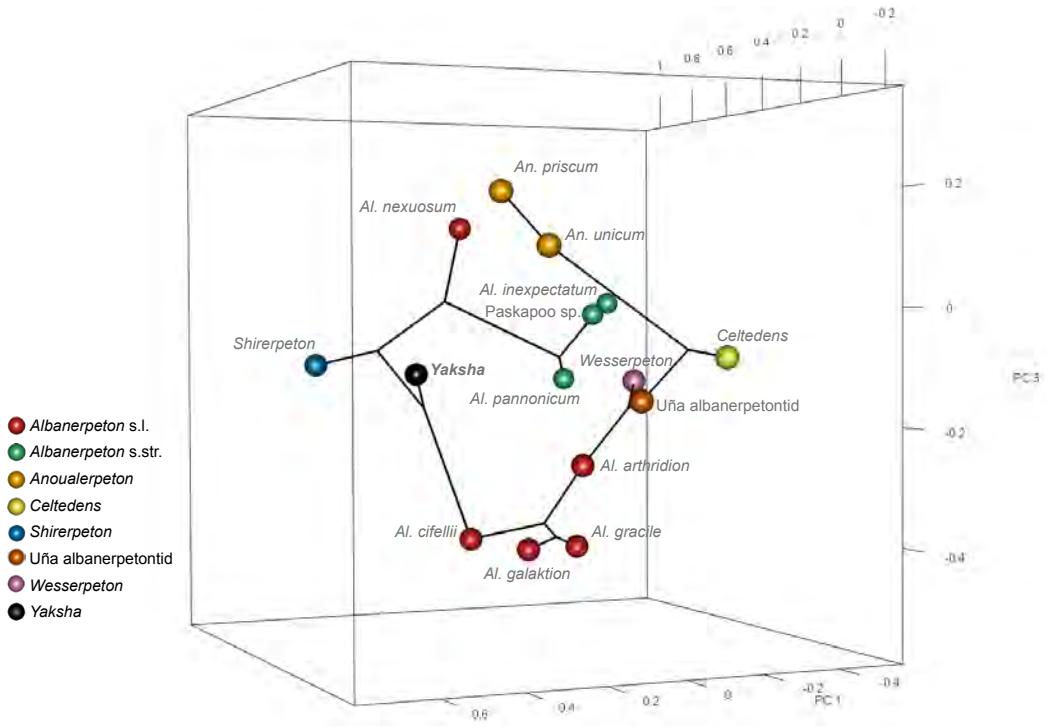

Fig. S11. 3D phylomorphospace for the matrix of albanerpetontids. Colors correspond to taxonomic groups.

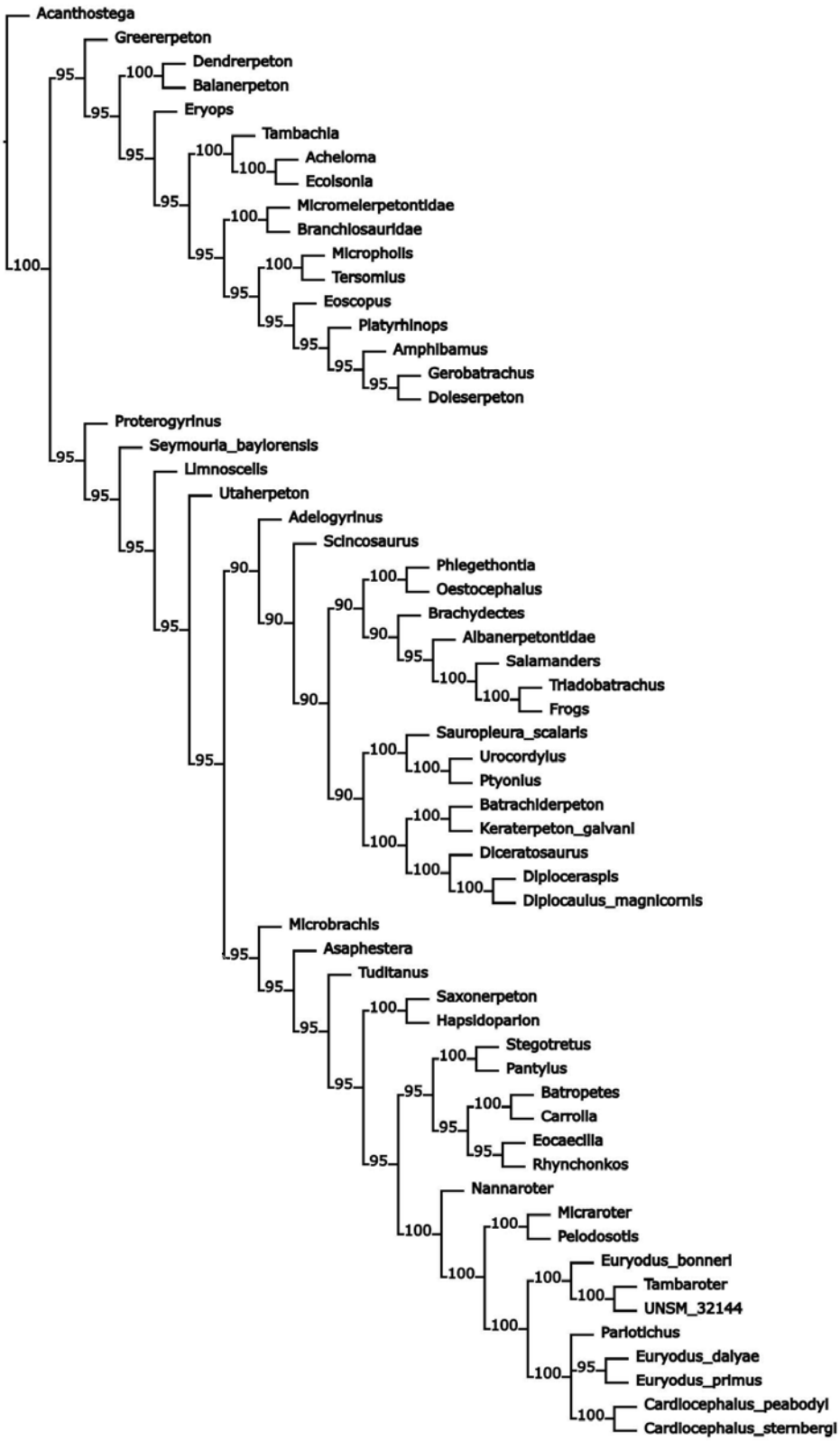

Fig. S12. Results of searches after adding data from *Yaksha* for albanerpetontids in the data set of Huttenlocker (*17*). Searches used implied weights, increasing the concavity value

using a size of class interval of 10 from 10 to 200. The tree is the majority rule representing all searches. Values on nodes indicate the percentage of that node being recovered when considering all analyses.

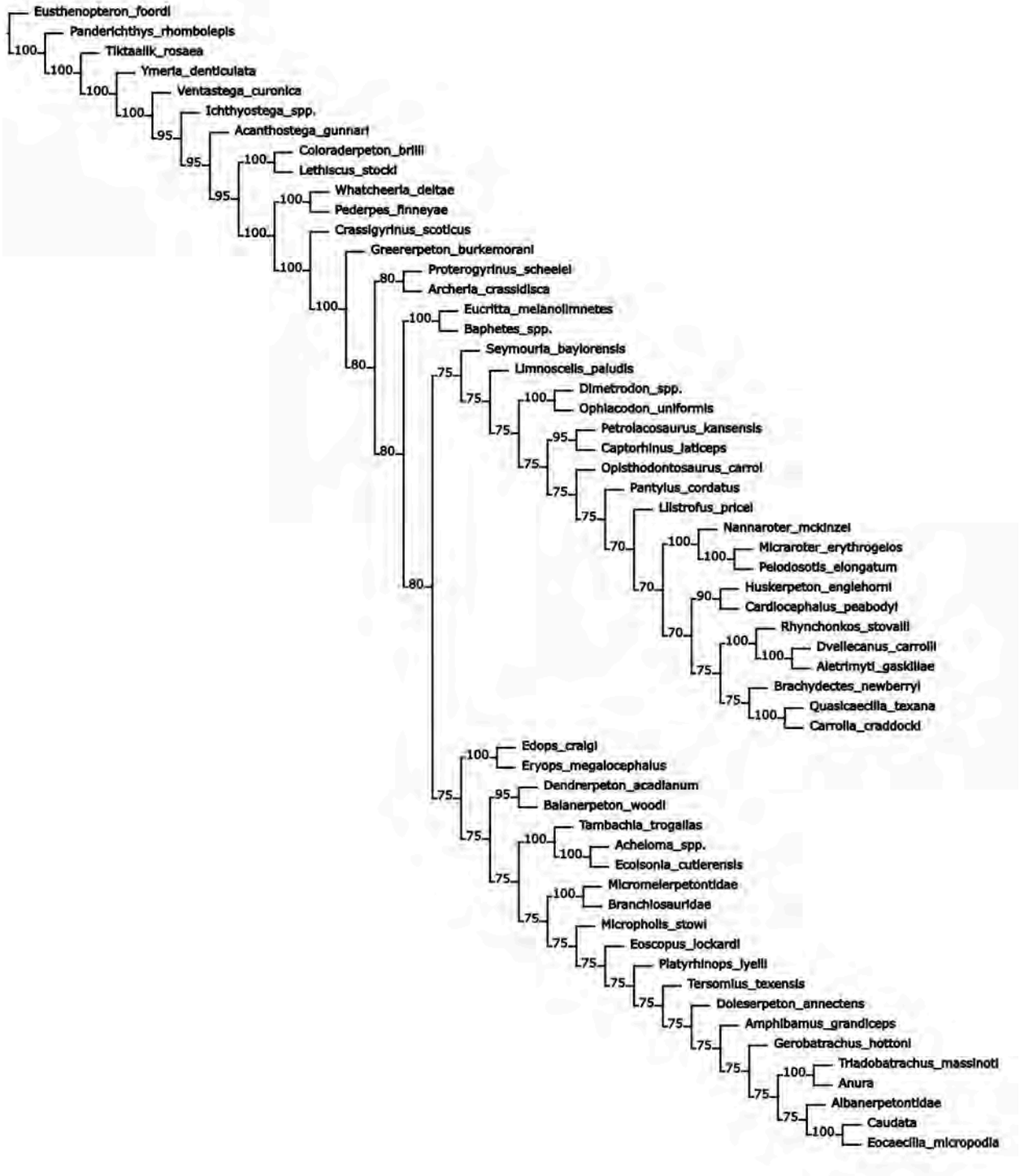

Fig. S13. Results of searches after adding data from *Yaksha* for albanerpetontids in the data set of Pardo et al.(*18*) with less representation for caecilians. Searches used implied weights, increasing the concavity value using a size of class interval of 10 from 10 to 200. The

tree is the majority rule representing all searches. Values on nodes indicate the percentage of that node being recovered when considering all analyses.

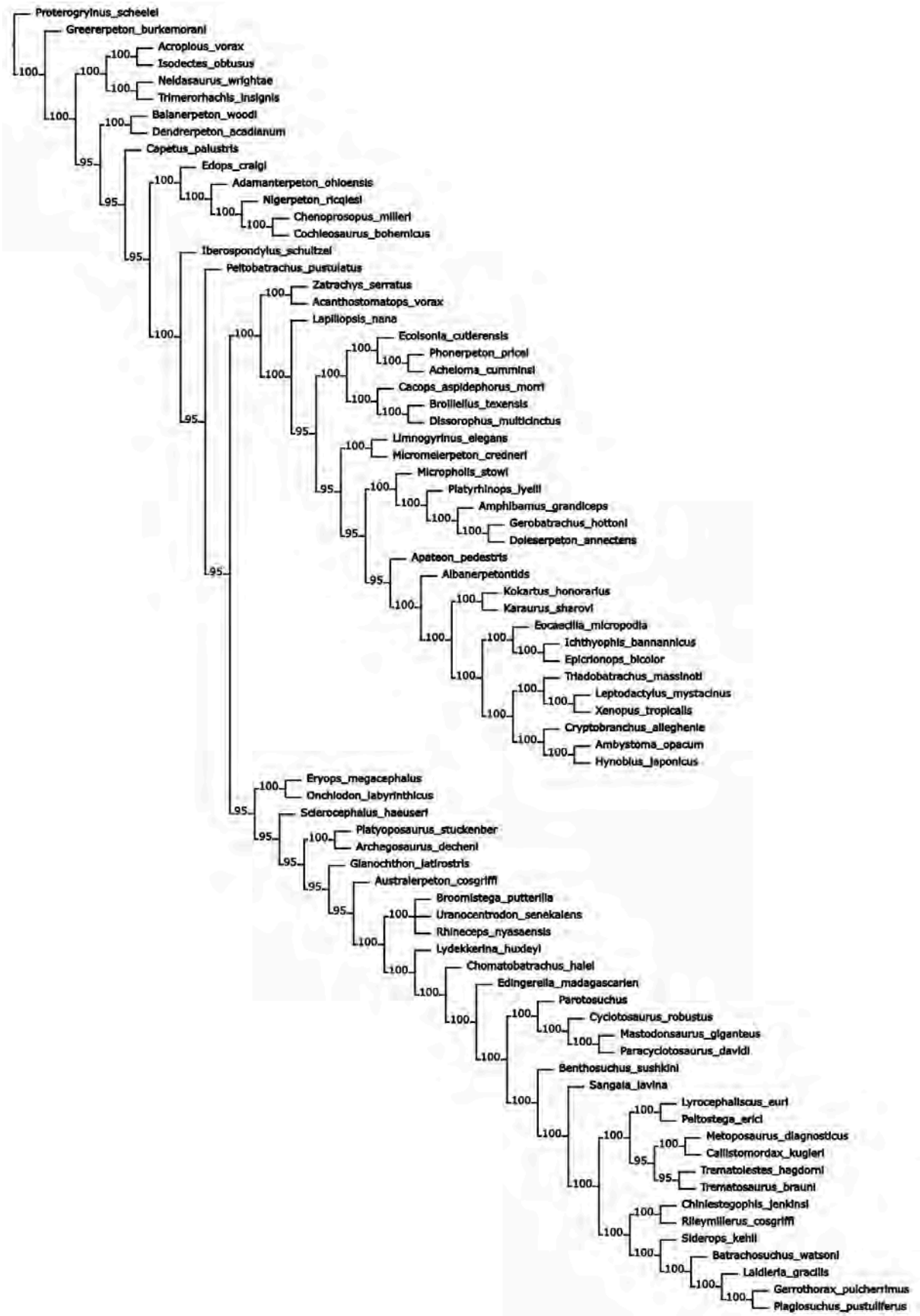
Proterogyrinus_scheelei
Greererpeton_burkemorani
Acroplous_vorax
Isodectes_obtusus
Neldasaurus_wrightae
Trimerorhachis_insignis
Balanerpeton_woodi
Dendrerpeton_acadianum
Capetus_palustris
Edops_craigi
Adamanterpeton_ohioensis
Nigerpeton_ricqlesi
Chenoprosopus_milleri
Cochleosaurus_bohemicus
Iberospondylus_schultzei
Peltobatrachus_pustulatus
Zatrachys_serratus
Acanthostomatops_vorax
Lapillopsis_nana
Ecolsonia_cutlerensis
Phonerpeton_pricei
Acheloma_cumminsi
Cacops_aspidephorus_morri
Broiliellus_texensis
Dissorophus_multicinctus
Limnogyrinus_elegans
Micromelerpeton_credneri
Micropholis_stowi
Platyrhinops_lyelli
Amphibamus_grandiceps
Gerobatrachus_hottoni
Doleserpeton_annectens
Apateon_pedestris
Albanerpetontids
Kokartus_honorarius
Karaurus_sharovi
Eocaecilia_micropodia
Ichthyophis_bannanicus
Epicrionops_bicolor
Rhadobatrachus_massinoti
Leptodactylus_mystacinus
Xenopus_tropicalis
Cryptobranchus_alleghenie
Ambystoma_opacum
Hynobius_japonicus
Eryops_megacephalus
Onchiodon_labyrinthicus
Sclerocephalus_haeuseri
Platyoposaurus_stuckenber
Archegosaurus_decheni
Glanochthon_latirostris
Australerpeton_cosgriffi
Broomistega_putterilli
Uranocentrodon_senekalens
Rhineceps_nyasaensis
Lydekkerina_huxleyi
Chomatobatrachus_halei
Edingerella_madagascarien
Parotosuchus
Cyclotosaurus_robustus
Mastodonsaurus_giganteus
Paracyclotosaurus_davidi
Benthosuchus_sushkini
Sangaia_lavina
Lyrocephaliscus_euri
Peltostega_erici
Metoposaurus_diagnosticus
Callistomordax_kugleri
Trematolestes_hagdorni
Trematosaurus_brauni
Chinlestegophis_jenkinsi
Rileymillerus_cosgriffi
Siderops_kehli
Batrachosuchus_watsoni
Laidleria_gracilis
Gerrothorax_pulcherrimus
Plagiosuchus_pustuliferus

Fig. S14. Results of searches after adding data from *Yaksha* for albanerpetontids in the data set of Pardo et al. (*19*) with more representation for caecilians. Searches used implied weights, increasing the concavity value using a size of class interval of 10 from 10 to 200. The tree is the majority rule representing all searches. Values on nodes indicate the percentage of that node being recovered when considering all analyses.

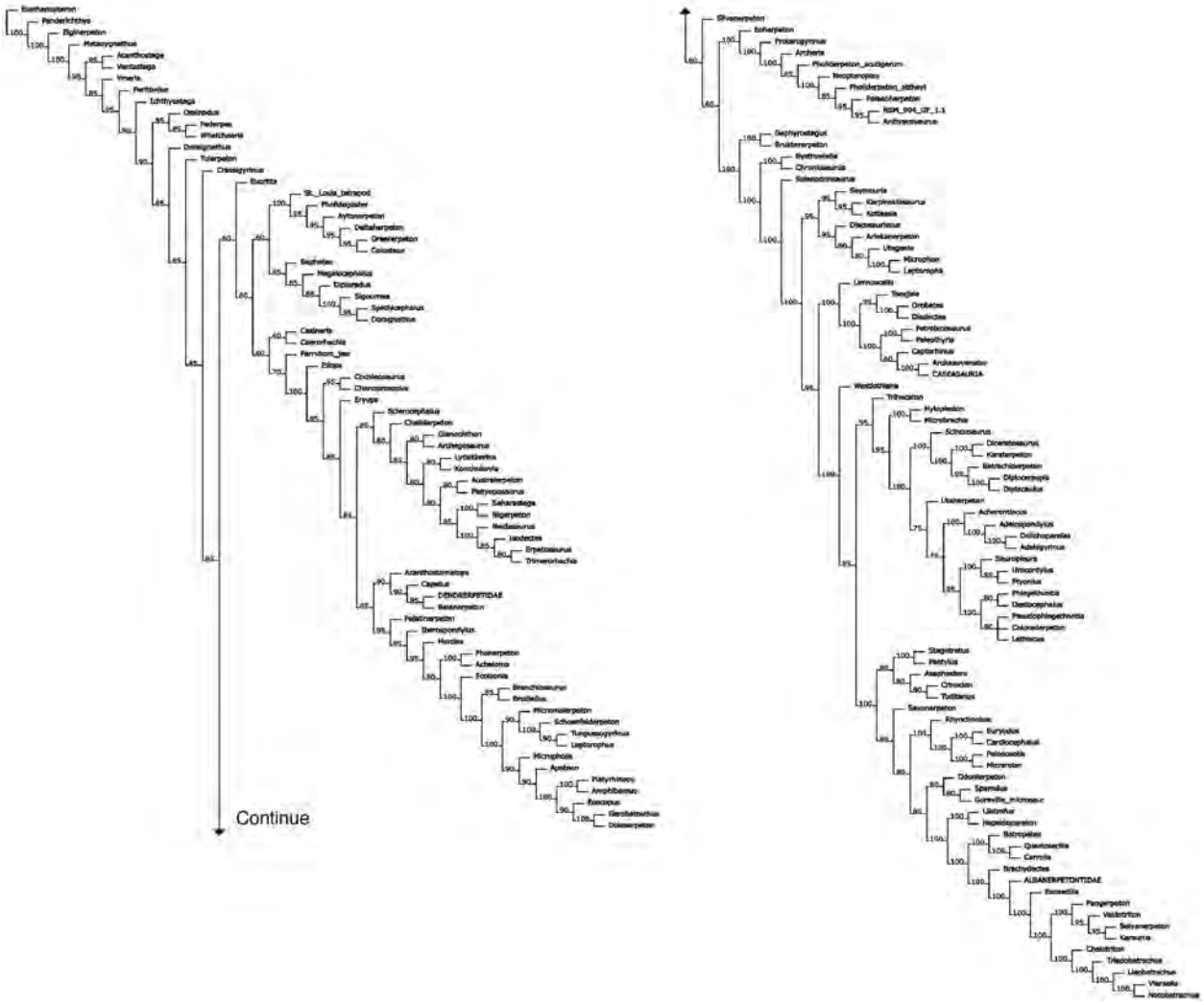

Fig. S15. Results of searches after adding data from *Yaksha* for albanerpetontids in the data set of Marjanović & Laurin(*20*). Searches used implied weights, increasing the concavity value using a size of class interval of 10 from 10 to 100. The tree is the majority rule representing all searches. Values on nodes indicate the percentage of that node being recovered when considering all analyses.